DRD1 Gaseous Detectors School

Modelling and Simulation 2

Djunes Janssens – CERN

Riccardo Farinelli – INFN sezione di Bologna

Dario Stocco – ETH Zurich

Piet Verwilligen - INFN sezione di Bari

djunes.janssens@cern.ch

December 2^{nd}, 2024

Outline

- **Simulating Gas Gain**
  - Average gain: Townsend coefficient and Penning transfer
  - Gain fluctuations: from toy-model to microscopic description
  - Garfield++ examples: Micromegas and µRWELL
  - Large avalanches: hydrodynamics approximation

- **Capacitive-coupling between electrodes**
  - Capacitance matrix: concept and numerical approach
  - Equivalent circuit description
  - Weighting potential description

- **Summary**

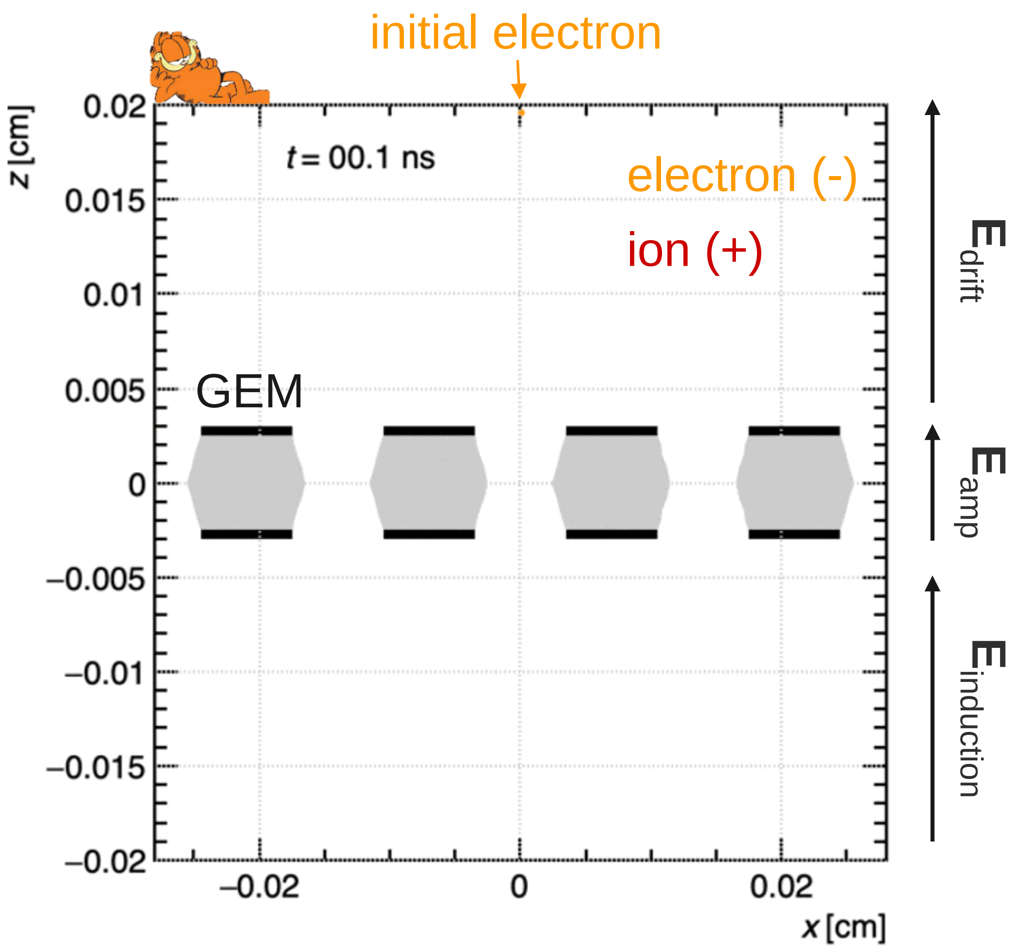

Outline

- **Simulating Gas Gain**
  - Average gain: Townsend coefficient and Penning transfer
  - Gain fluctuations: from toy-model to microscopic description
  - Garfield++ examples: Micromegas and µRWELL
  - Large avalanches: hydrodynamics approximation
- **Capacitive-coupling between electrodes**
  - Capacitance matrix: concept and numerical approach
  - Equivalent circuit description
  - Weighting potential description
- **Summary**

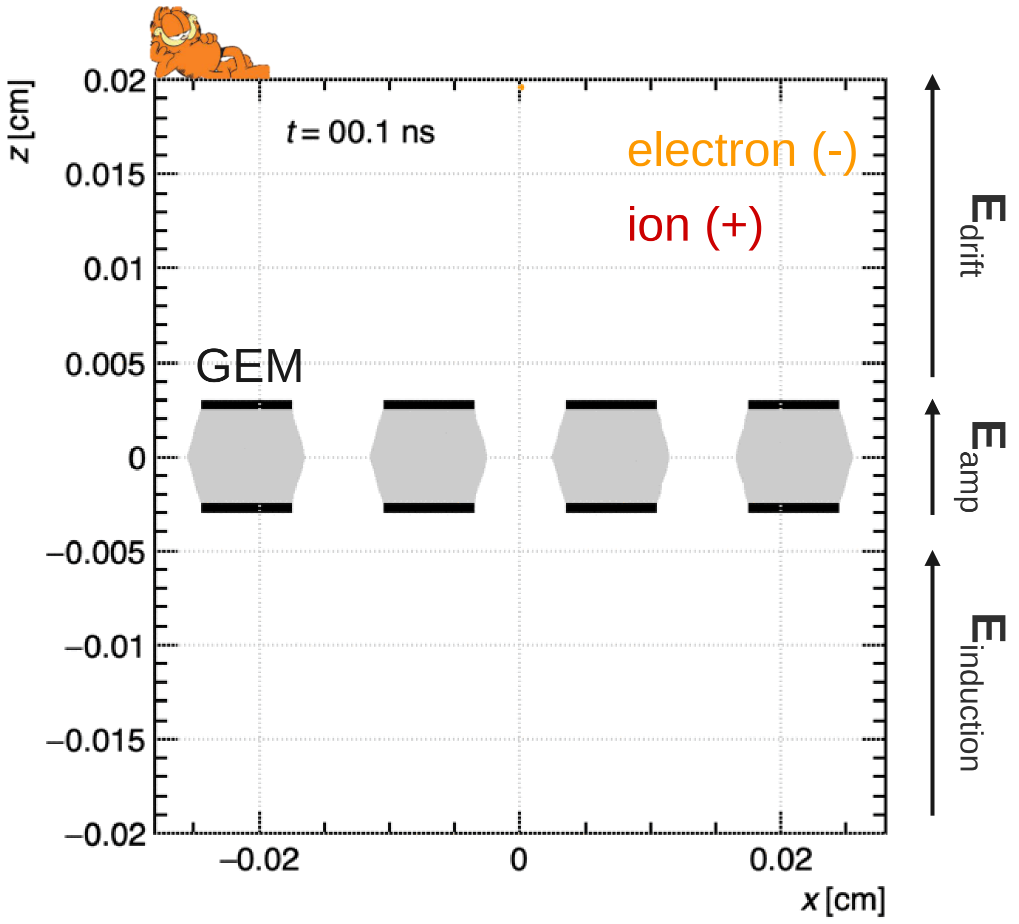

Average Gas Gain

Gas Multiplication

The amount of charge produced by a charged particle crossing a gas detector is usually too small to be measured directly, 40 e^- ≈ 6.4×10^{-3} fC.

The number of electrons produced by N electrons traversing an interval dx is:

$$dN = \alpha N dx$$
$$\Rightarrow N = N_0 e^{\alpha x}$$

When the electric field is not uniform, we will find at position s on average:

$$N(s) = N_0 \exp \int_0^s \alpha\left(s'\right) ds'$$

Sir John Sealy Edward Townsend
(1868-1957)

J.S. Townsend, “The conductivity produced in gases by the motion of negatively charged ions”, Phil. Mag. 6-1 (1901) 198-227.
If access to the Philosophical Magazine is restricted, then consult a German-language abstract at http://jfm.sub.uni-goettingen.de/.

Gas Multiplication

The Townsend coefficient is the number of e^- created per cm.

This coefficient is determined by the excitation and ionization cross-sections of the atoms and molecules inside the gas.

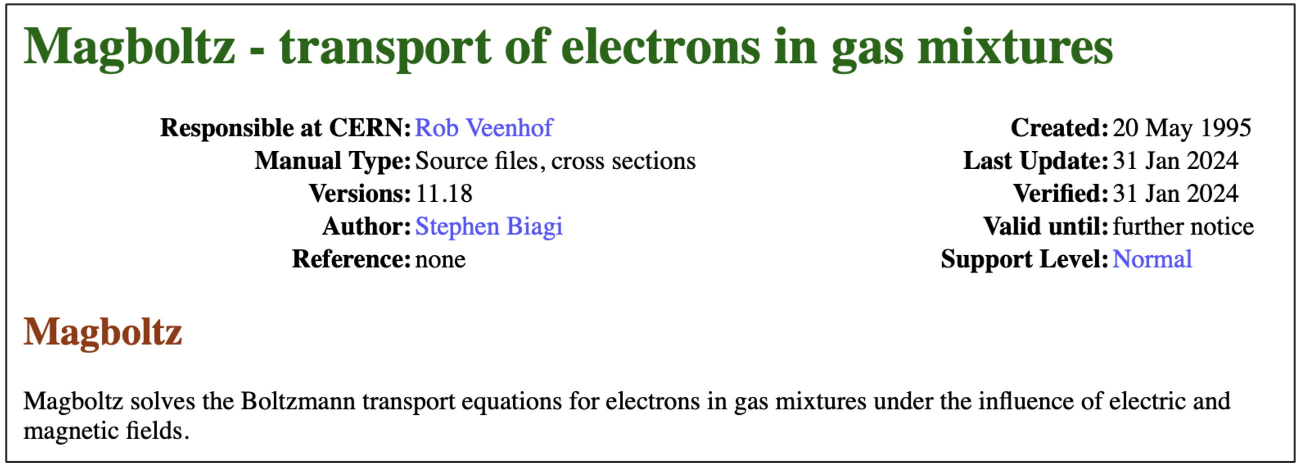

Magboltz - transport of electrons in gas mixtures

Responsible at CERN: Rob Veenhof
Manual Type: Source files, cross sections
Versions: 11.18
Author: Stephen Biagi
Reference: none

Created: 20 May 1995
Last Update: 31 Jan 2024
Verified: 31 Jan 2024
Valid until: further notice
Support Level: Normal

Magboltz

Magboltz solves the Boltzmann transport equations for electrons in gas mixtures under the influence of electric and magnetic fields.

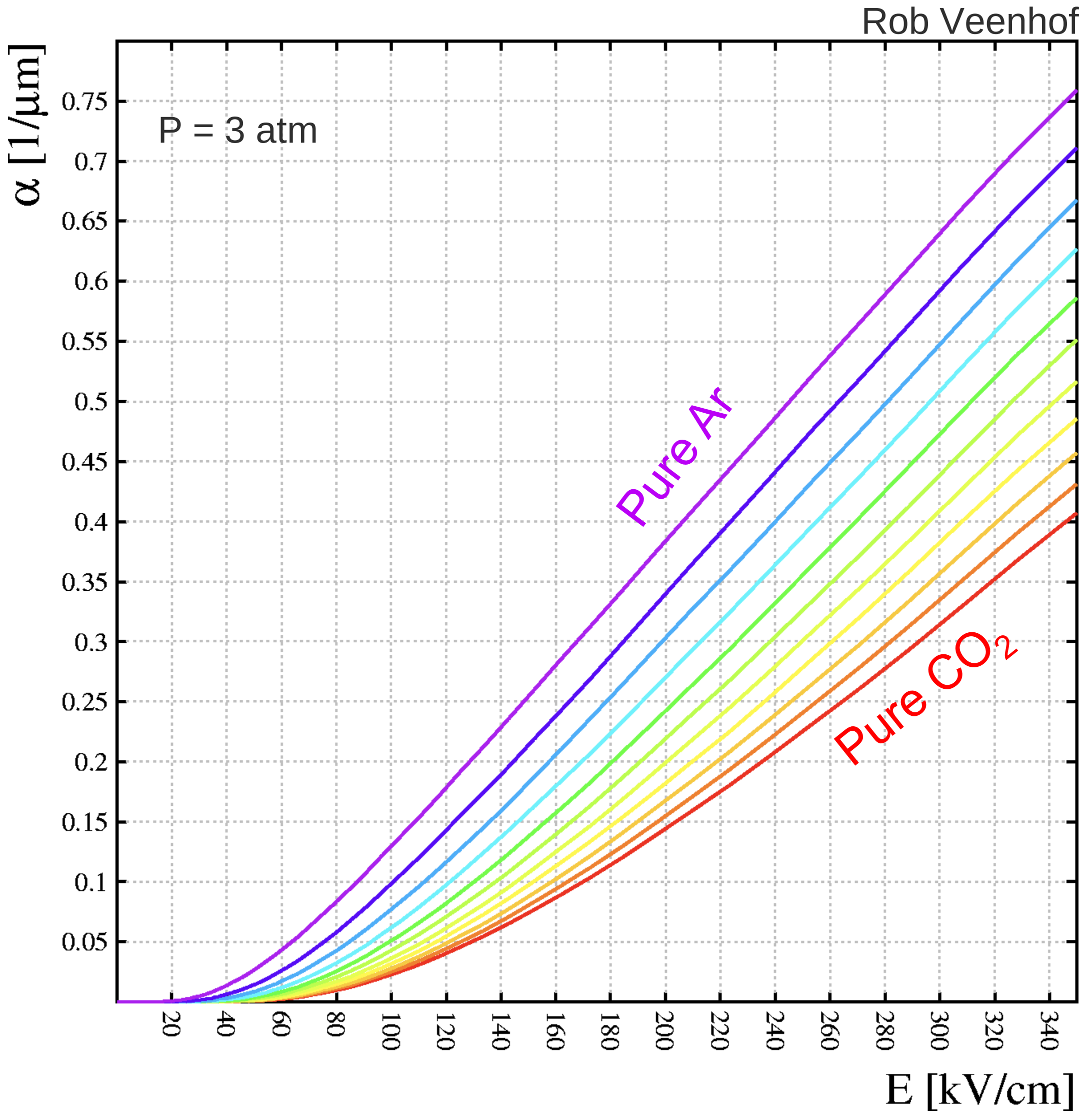

Gas Multiplication

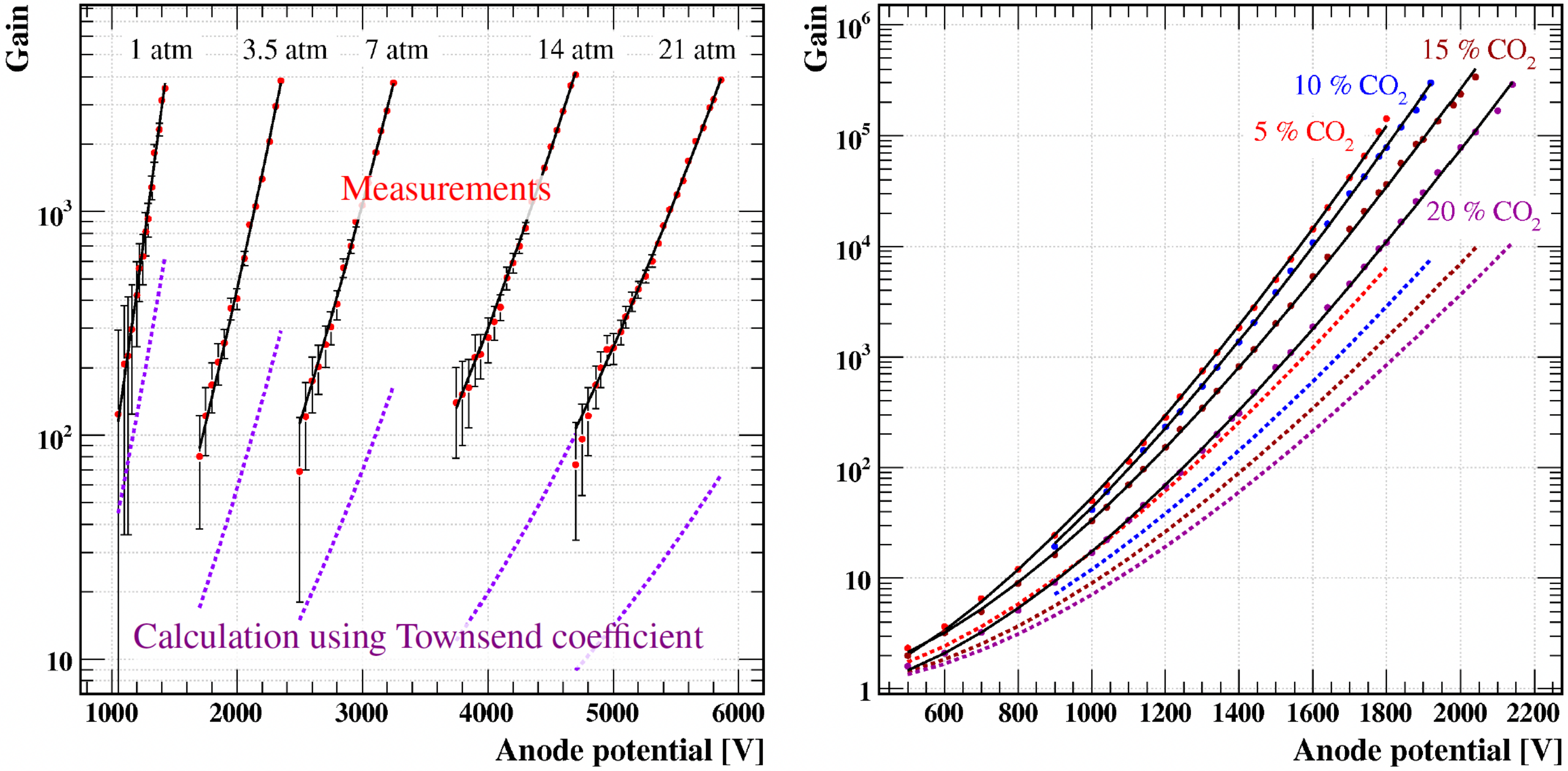

Argon Cross-sections

Rob Veenhof

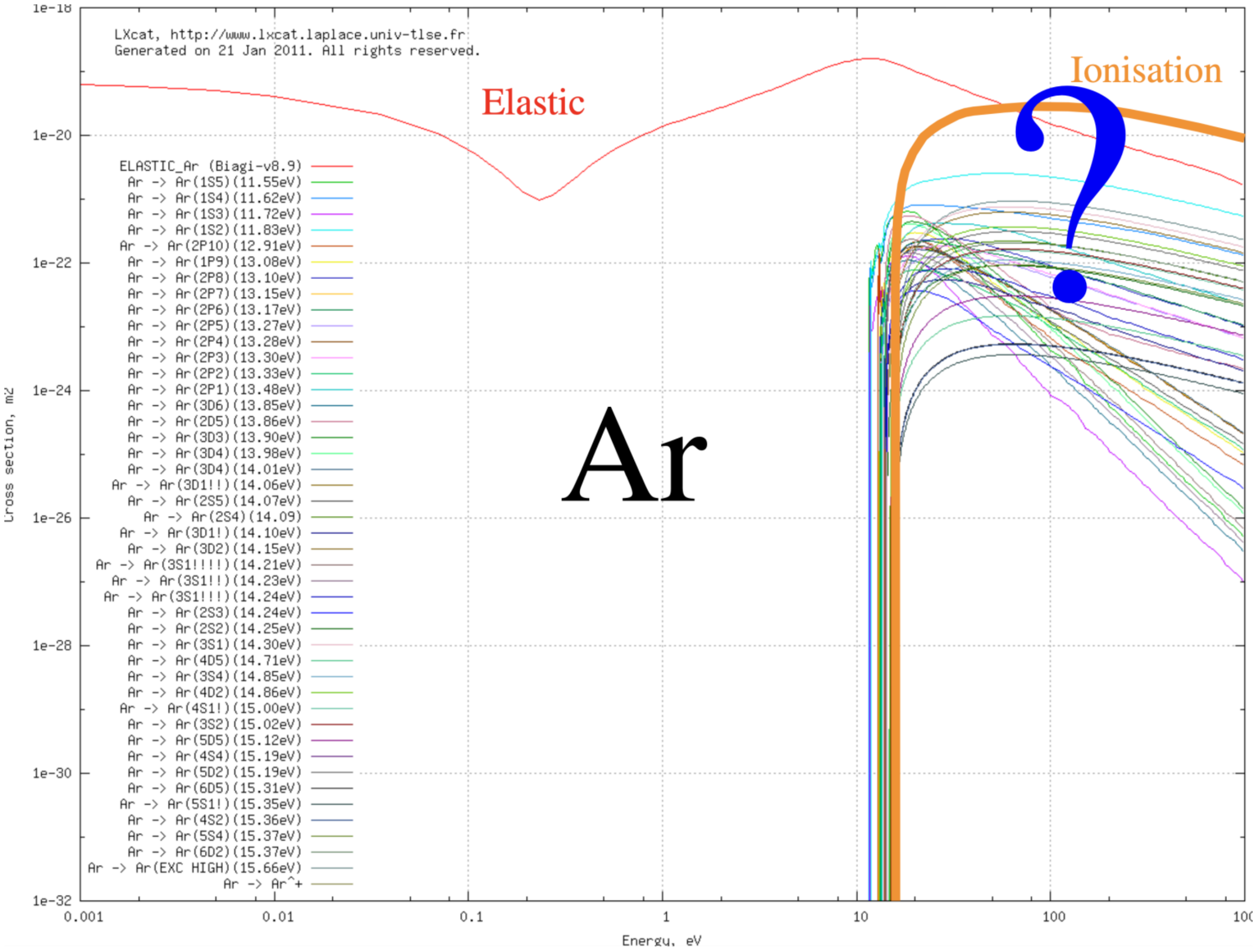

Penning Transfer

Frans Michel Penning
(1894-1953)

Excitations represent a significant scattering process at high electron energies. Argon has excited states above the ionization energy of typical admixtures, including CO_2.

Excimer formation:

$$A^\star + 2A \to A_2^\star + A$$

Photon-induced excitation transfer:

$$A^\star \to A + \gamma, \qquad B + \gamma \to B^+ + e^-$$

Collision-induced excitation transfer:

$$A^\star + B \to A + B^+ + e^-$$

Homonuclear associative ionization:

$$A^{\star\star} + A \to A_2^+ + e^-$$

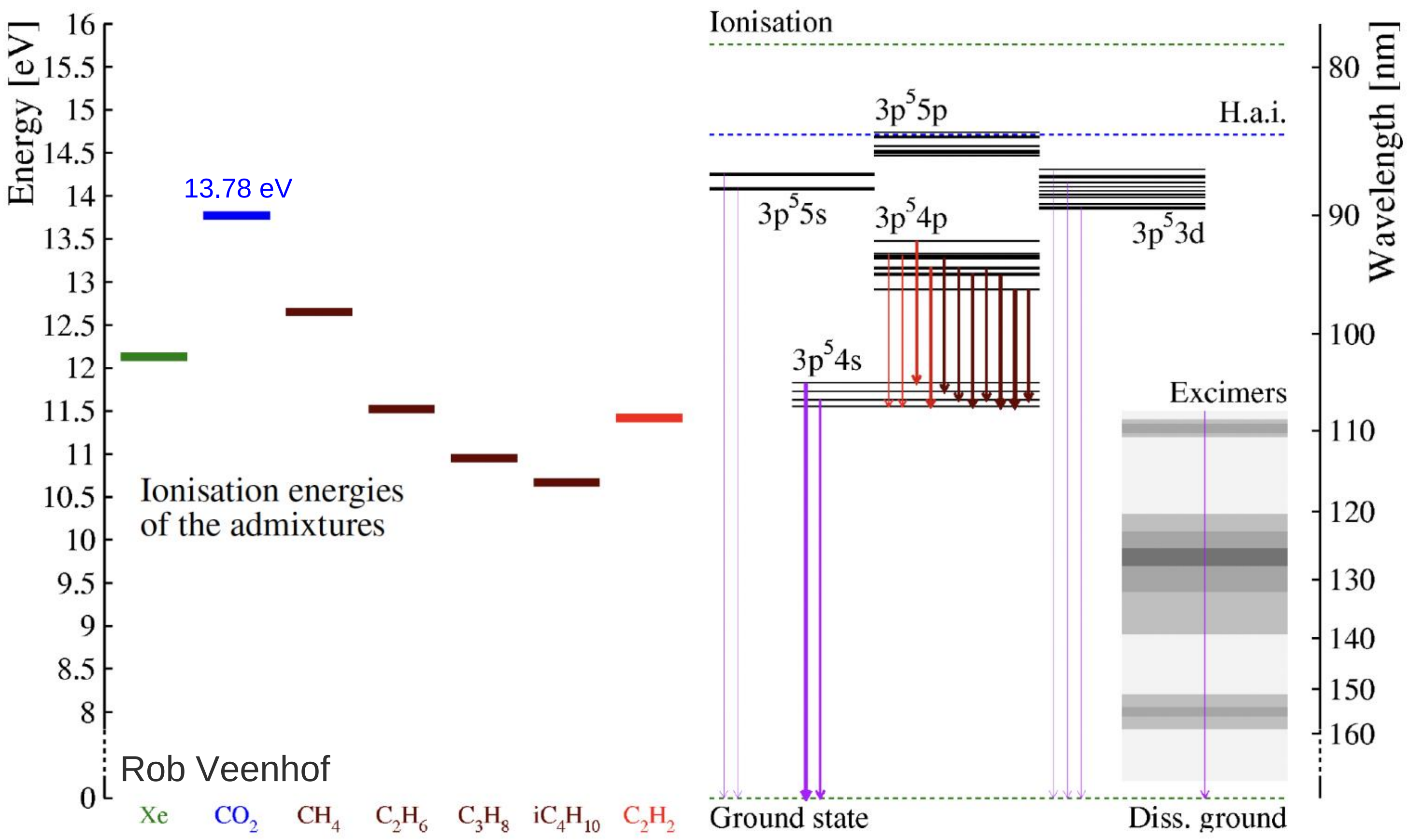

Penning Transfer

As such, the Townsend coefficient needs to be corrected:

$$\alpha' = \alpha\left(1 + r_\mathrm{P}\frac{\nu^{exc}}{\nu^{ion}}\right)$$

, where

fraction of CO_2

$$r_\mathrm{P} = \frac{pc\frac{f_{B+}}{\tau_{A^*B}} + \frac{f_{rad}}{\tau_{A^*}}}{pc\frac{f_{B+}+f_{\bar{B}}}{\tau_{A^*B}} + \frac{1}{\tau_{A^*}}}$$

Ar/CO_2	NIM A 768 (2014), 104	$r_\mathrm{P}(c)$ at atmospheric pressure
Ar/CO_2	JINST 12 (2017), C01035	$r_\mathrm{P}(c, p)$
Ar/CH_4	JINST 5 (2010), P05002	$r_\mathrm{P}(c, p)$
Ar/C_2H_6	JINST 5 (2010), P05002	r_P for 10% C_2H_6 at atmospheric pressure
Ar/C_3H_8	JINST 5 (2010), P05002	$r_\mathrm{P}(c)$ at atmospheric pressure
Ar/iC_4H_{10}	JINST 5 (2010), P05002	r_P for 10% iC_4H_{10} at atmospheric pressure
Ar/C_2H_2	JINST 5 (2010), P05002	r_P at atmospheric pressure
Ar/Xe	JINST 5 (2010), P05002	$r_\mathrm{P}(c)$ at atmospheric pressure
Ne/CO_2	JINST 16 (2021), P03026	$r_\mathrm{P}(c, p)$
Ne/N_2	JINST 16 (2021), P03026	$r_\mathrm{P}(c, p)$
Xe/TMA	JINST 13 (2018), P10032	$r_\mathrm{P}(p)$ for 5% TMA

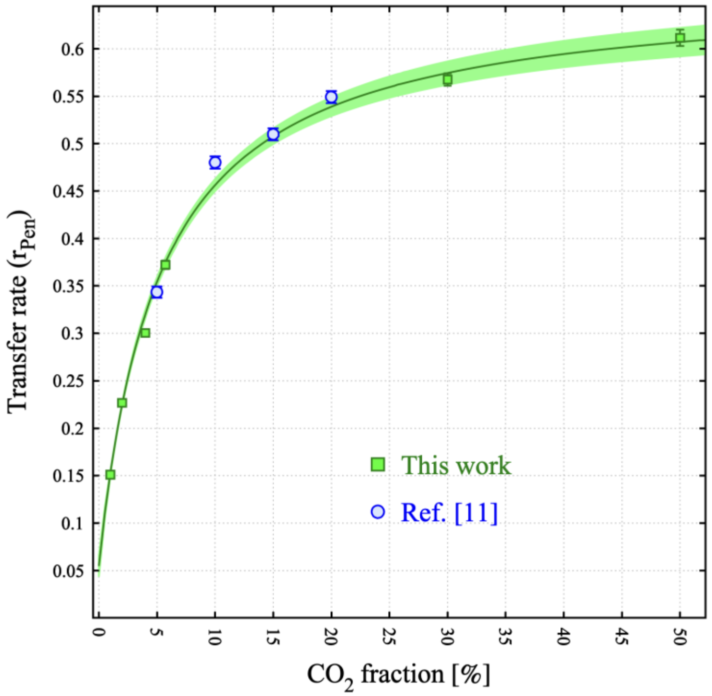

Example: Parallel Plate

Let us consider a Townsend avalanche inside the amplification gap of a Micromegas detector that induces a signal on the anode plane.

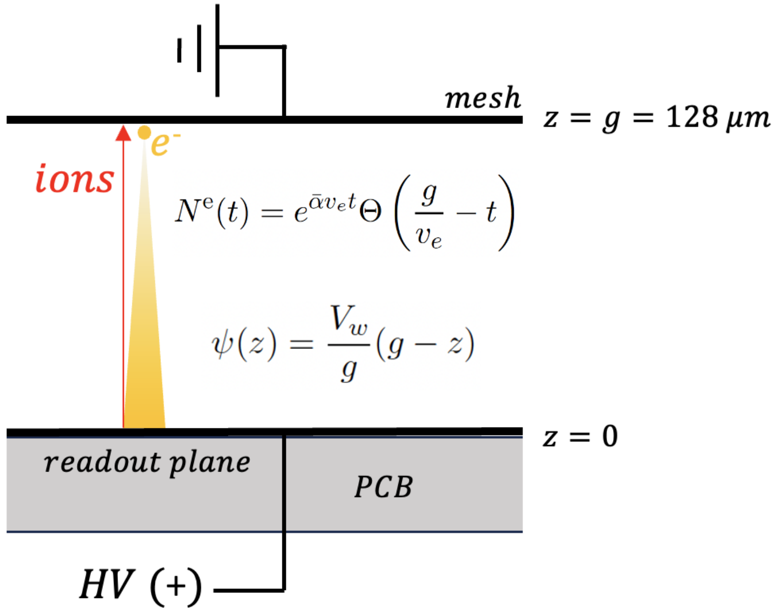

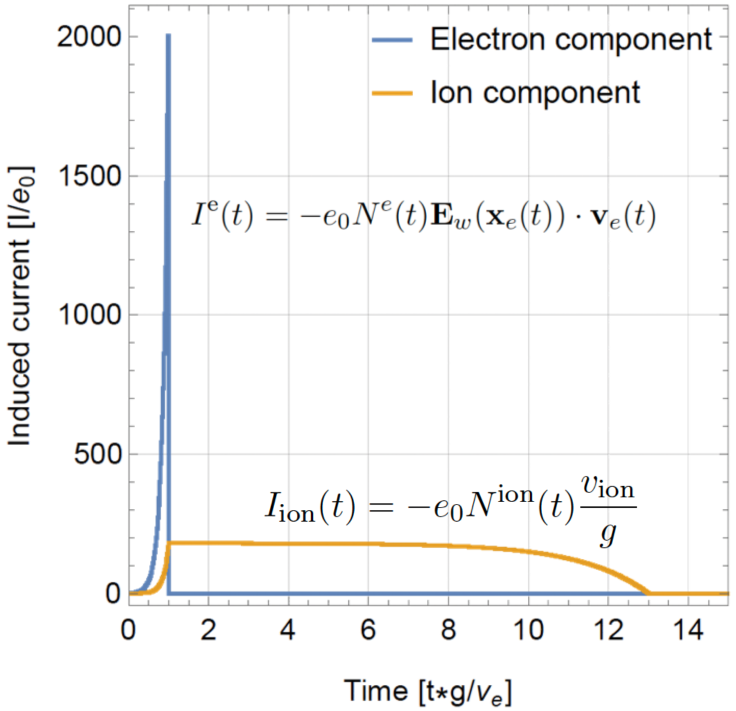

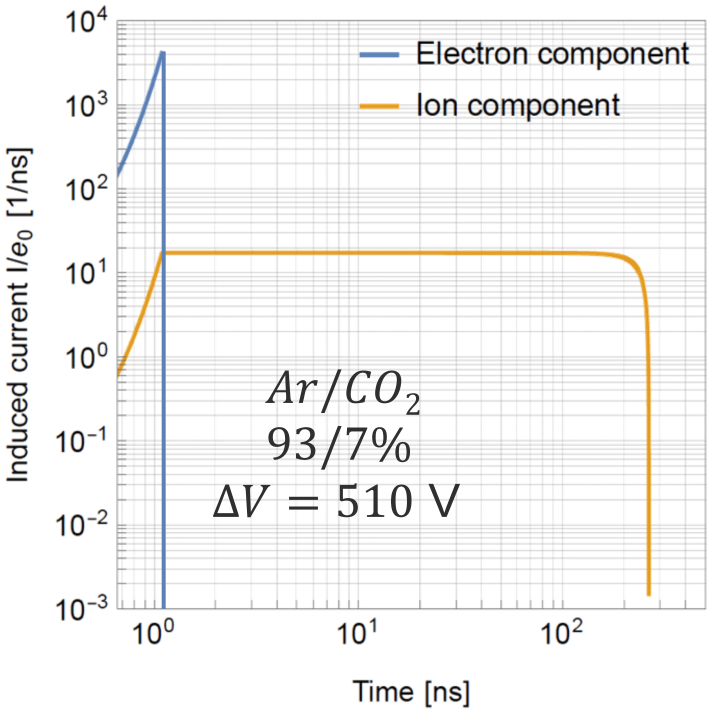

Statistical Fluctuation of the Gain

Avalanche Size Distribution

The avalanche size distribution in strong homogeneous fields was measured by Schlumbohm (1958) for parallel-plate geometry in methylal vapor at five different fields of increasing strength.

Townsend coef.

Ionization potential

$$\chi = \frac{\alpha(E)U_i}{E}$$

electric field

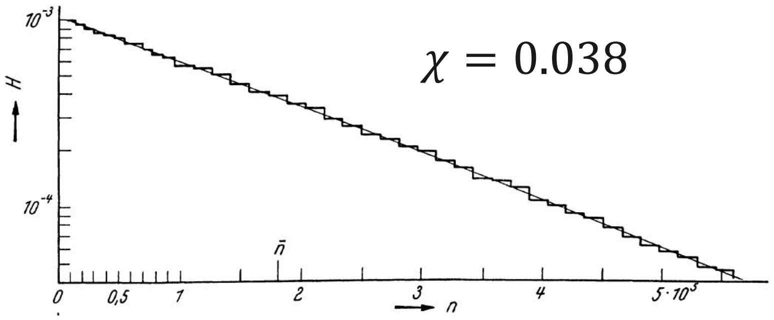

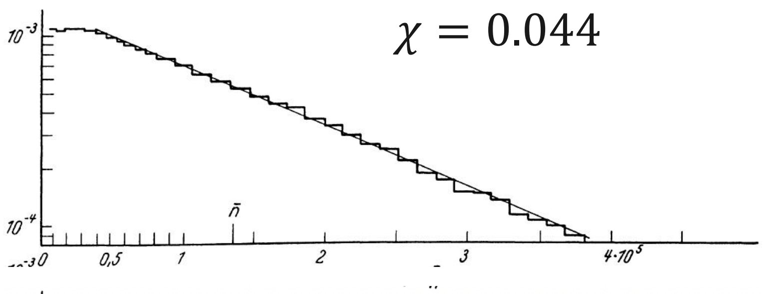

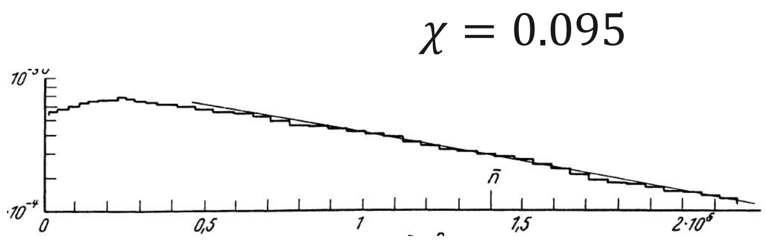

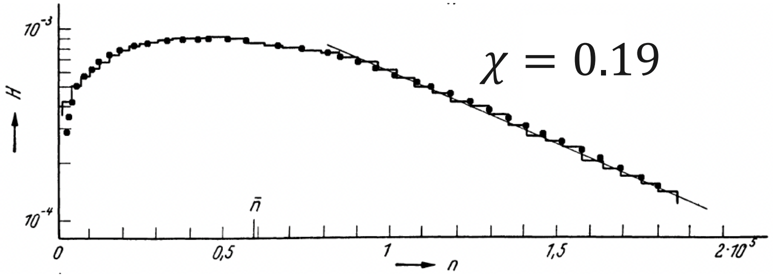

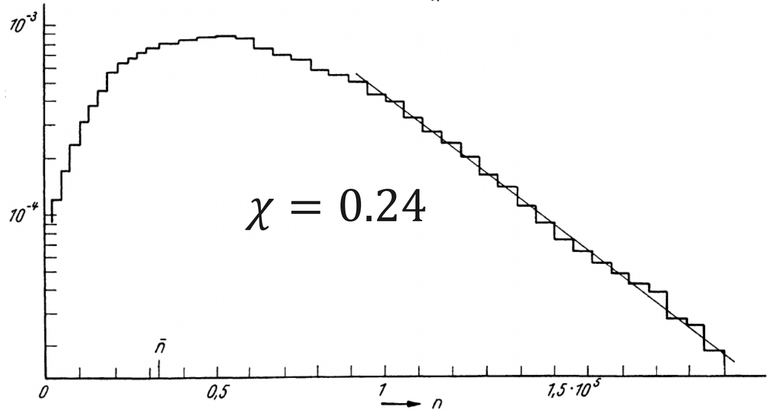

H. Schlumbohm, Z. Phys. 151 (1958) 563.

Avalanche Size Distribution

George Udny Yule
(1871-1951)

Assuming that the distance between successive ionizing collisions of an electron is exponentially distributed with a mean free path $\lambda = \alpha^{-1}$ independent of the electron energy, we have:

$$P_n(x+dx) = [1 - n\alpha(x)dx]P_n(x) + (n-1)\alpha(x)dxP_{n-1}(x) + \mathcal{O}\left(dx^2\right)$$

Probability that the avalanche reaches n electrons after a distance x+dx, starting with 1 e$^-$.

The solution to the above equation is given by

$$P_n\left(x\right) = \frac{1}{\overline{n}}\left(1 - \frac{1}{\overline{n}}\right)^{n-1}$$

, where

$$\overline{n} = \exp\left(\int_0^x \alpha\left(s\right) \mathrm{d}s\right)$$

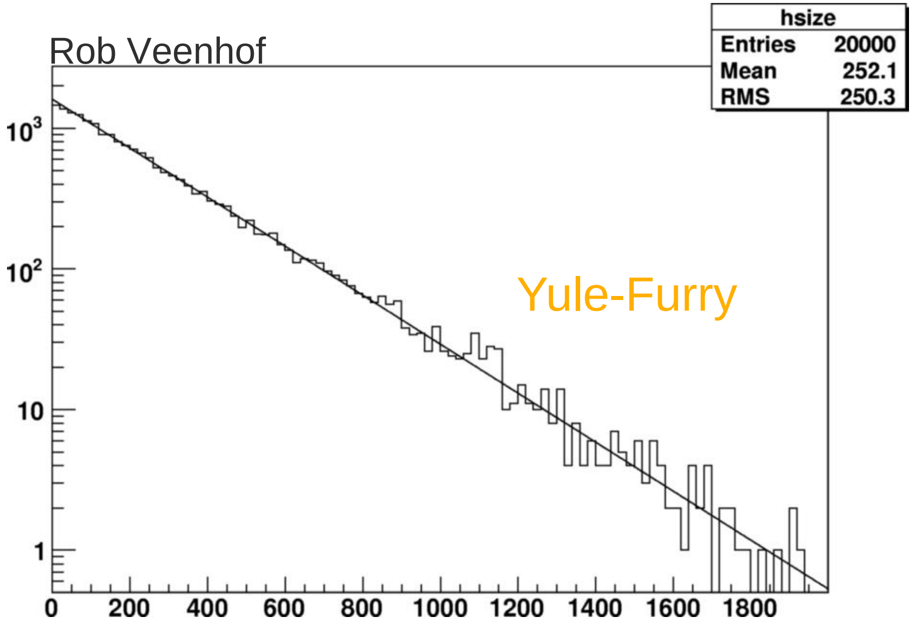

G. Udny Yule, A Mathematical Theory of Evolution, based on the Conclusions of Dr. J.C. Willis, F.R.S., Phil. Trans. Roy. Soc. London B 213 (1925) 21-87.
W.H. Furry, On Fluctuation Phenomena in the Passage of High Energy Electrons through Lead, Phys. Rev. 52 (1937) 569-581.

Robert A. Wijsman, Breakdown Probability of a Low Pressure Gas Discharge, Phys. Rev. 75 (1949) 833-838.

Avalanche Size Distribution

As straightforward extensions of the Yule-Furry model, we can introduce an attachment coefficient η in addition to the Townsend coefficient.

$$\begin{aligned} P_n(x+\mathrm{d}x) = & P_{n-1}(x)(n-1)\alpha(x)\mathrm{d}x[1-(n-1)\eta(x)\mathrm{d}x] \\ & + P_n(x)[1-n\alpha(x)\ \mathrm{d}x][1-n\eta(x)\ \mathrm{d}x] \\ & + P_n(x)n\alpha(x)\ \mathrm{d}xn\eta(x)\ \mathrm{d}x \\ & + P_{n+1}(x)[1-(n+1)\alpha(x)\mathrm{d}x](n+1)\eta(x)\mathrm{d}x \end{aligned}$$

For a uniform electric field, Legler showed that at first order the solution is

$$P_n(x) = \begin{cases} \frac{\eta}{\alpha}\frac{\overline{n}-1}{\overline{n}-\eta/\alpha}, & n=0 \\ \overline{n}\left(\frac{1-\eta/\alpha}{\overline{n}-\eta/\alpha}\right)^2\left(\frac{\overline{n}-1}{\overline{n}-\eta/\alpha}\right)^{n-1}, & n>0 \end{cases}$$

where

$$\overline{n} = \mathrm{e}^{(\alpha-\eta)x}$$

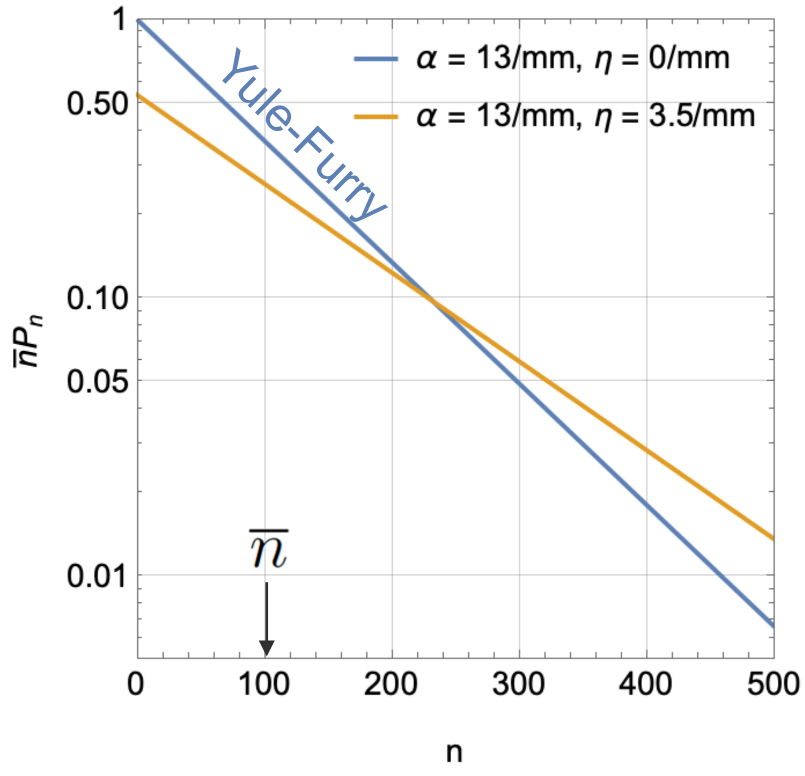

W. Legler, Z. Naturforschung. 16a (1961) 253.

Example: Resistive Plate Chamber

The gas gap of an RPC can be partitioned into a lattice, on which the avalanche is propagated towards the anode.

For each step, a Monte-Carlo simulation is performed to simulate the growth of the avalanche.

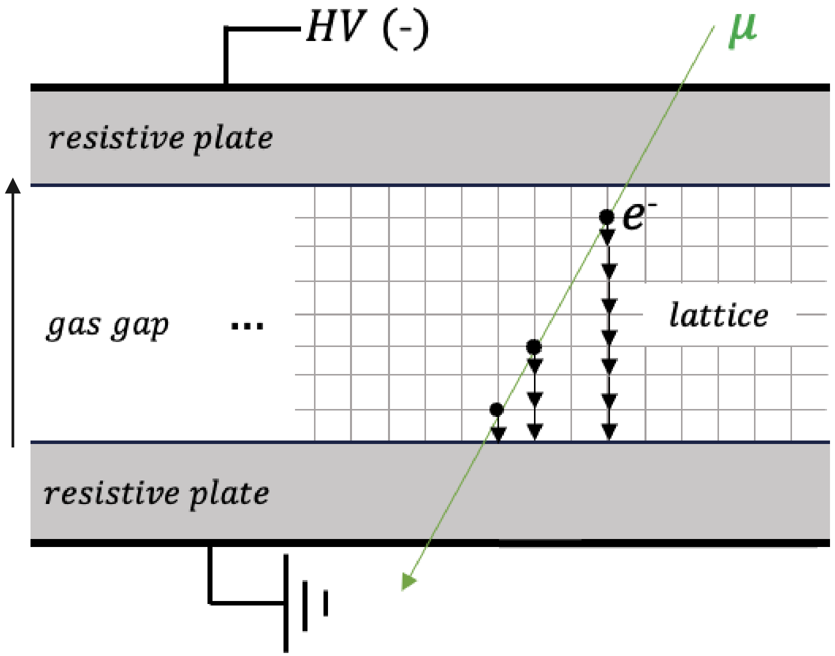

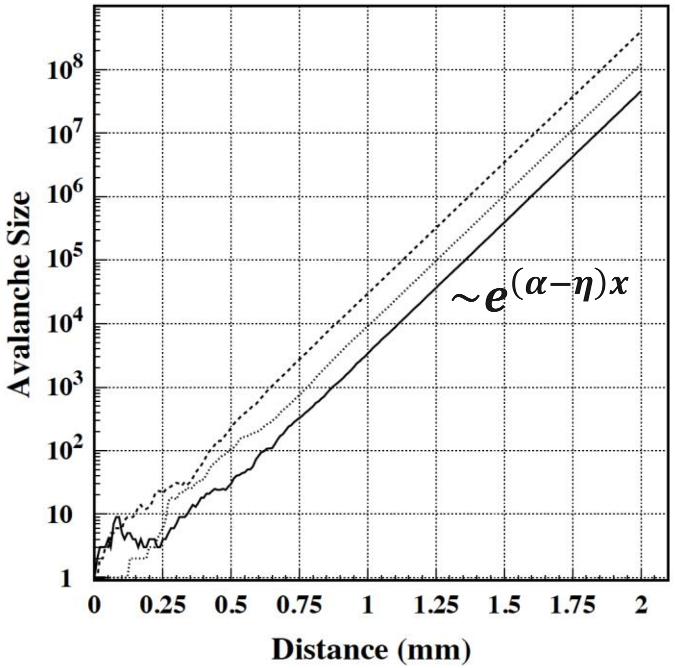

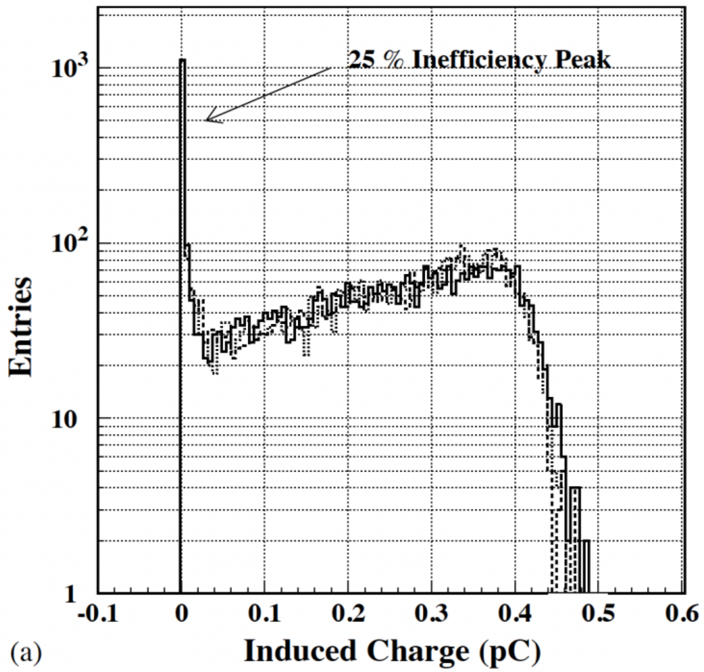

Avalanche Size Distribution

W. Legler emphasized that electrons need to travel a minimum distance along the electric field before they can ionize.

Imposing a minimum distance between ionizations creates a rounding to the initial part of the avalanche size spectrum!

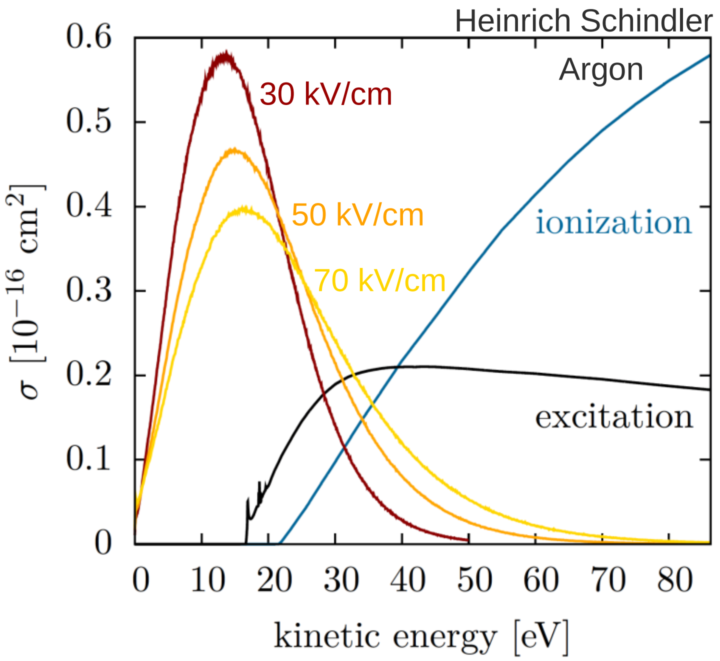

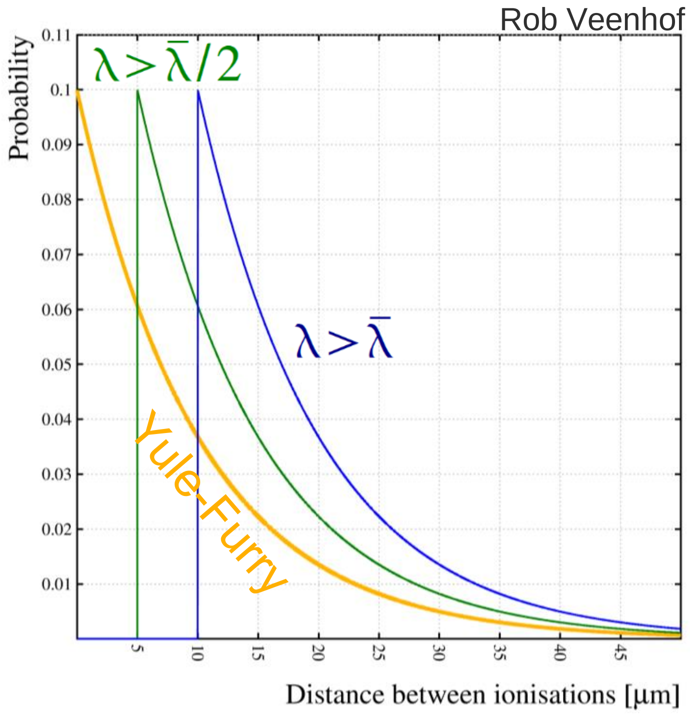

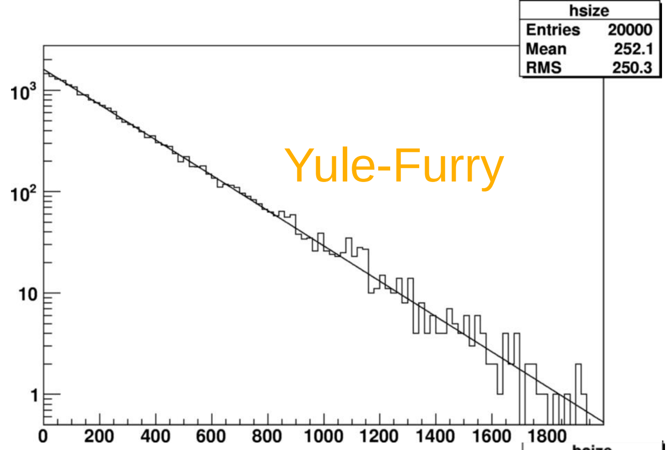

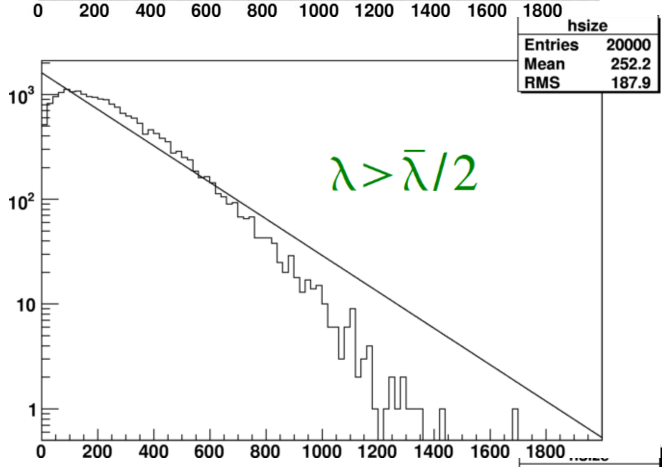

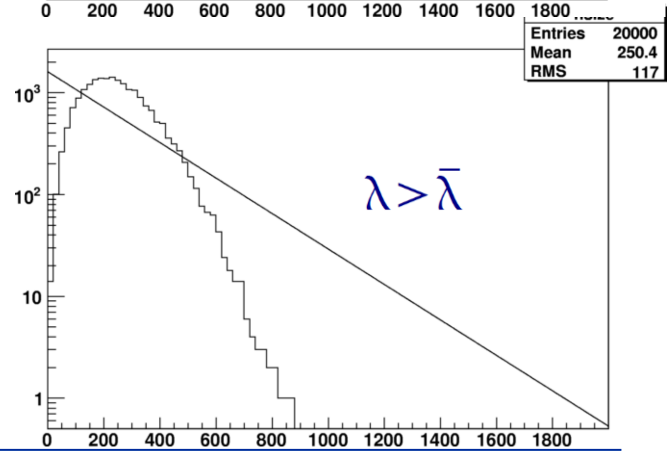

G. U. Yule, Phil. Trans. R. Soc. London B 213, 21 (1924).
W. H. Furry, Phys. Rev. 52, 569 (1937).
An overview of avalanche models: G. D. Alkhazov, Nucl. Instr. Meth. 89, 155 (1970).

Microscopic Model

The simulation method is based on the Monte-Carlo transport algorithm from the Magboltz program, utilizing its electron-molecule cross-section database.

Simplified description:

1. Null-collision method is used to determine the time until collision
2. Determine the relative probabilities of collisional processes
3. Check which of the available collisional process occurred
4. Update electron energy (and create new electron-ion pair)

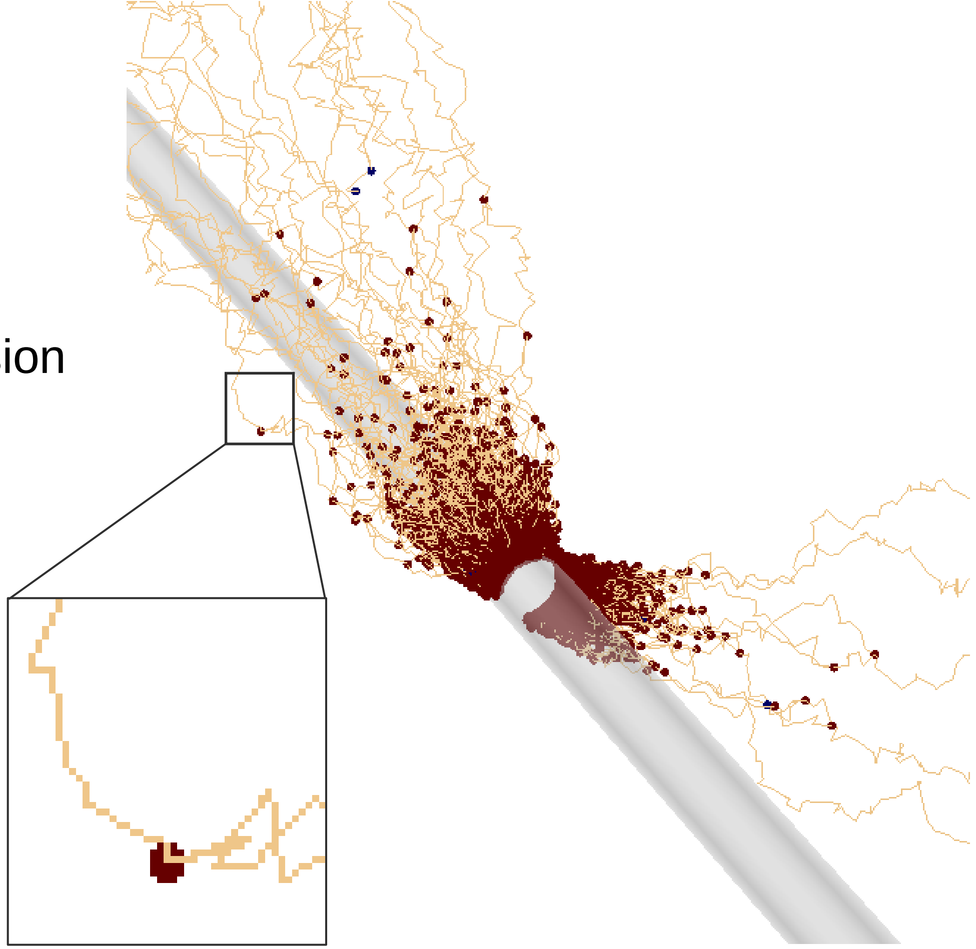

H. R. Skullerud, J. Phys. D 1, 1567 (1968).
S. F. Biagi, NIM-A 421 (1999) 234.
H. Schindler, S.F. Biagi, R. Veenhof, NIM-A 624(2010)78–84.

Microscopic Model

Using this description, the distribution of the distance ξ that electros travel between successive ionizing collisions can be obtained. Compared to Methane, Argon ξ exhibits distinct bumps at regular intervals.

Magboltz calculation by Heinrich Schindler

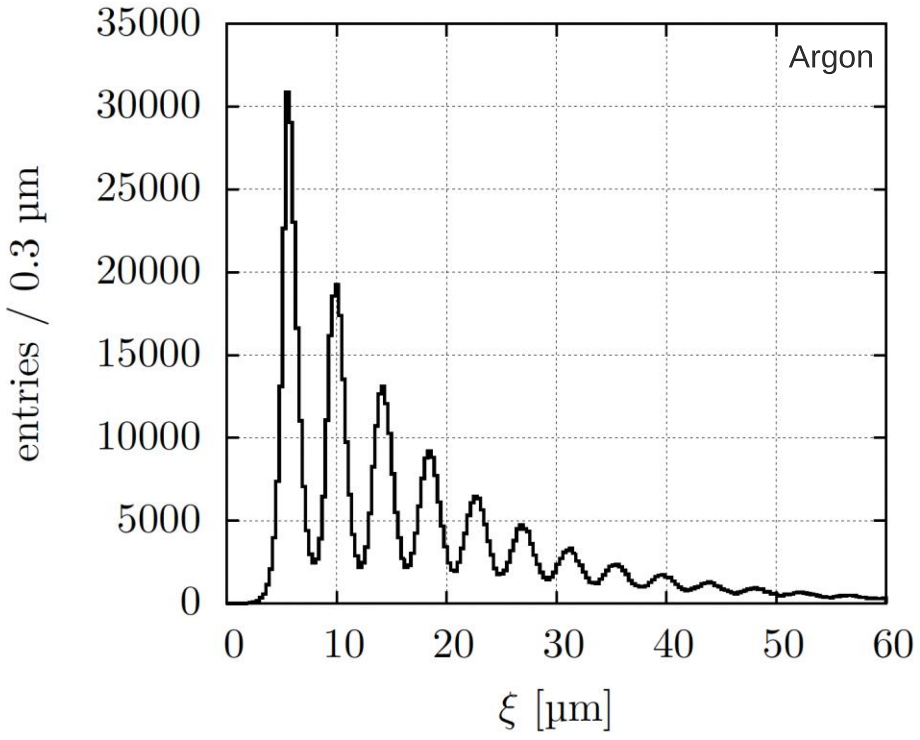

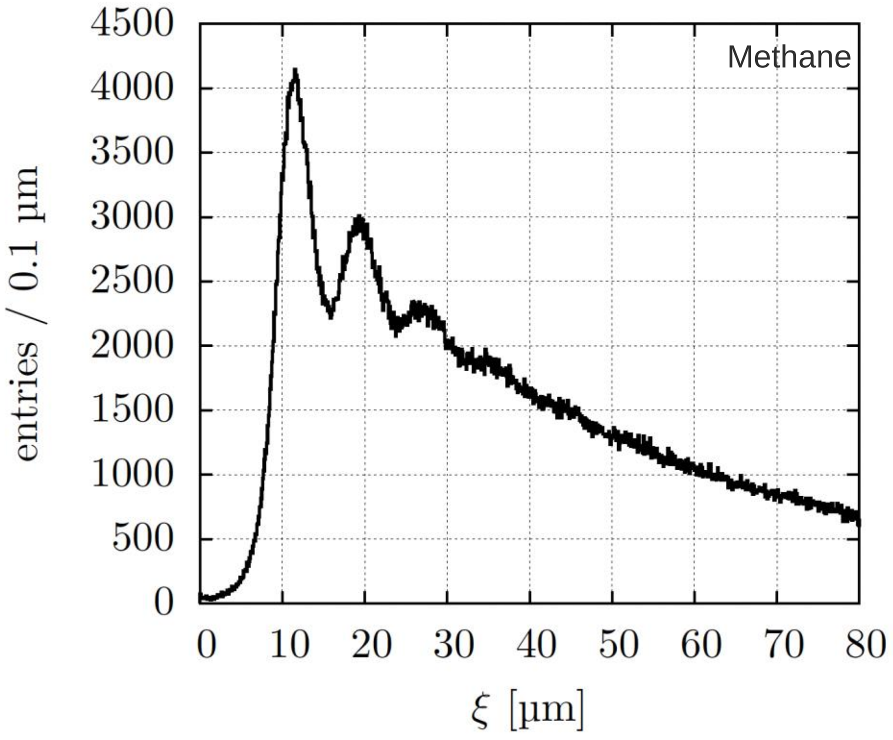

Images taken from: H. Schindler, S.F. Biagi, R. Veenhof, NIM-A 624 (2010) 78–84.

Argon Cross-sections

Rob Veenhof

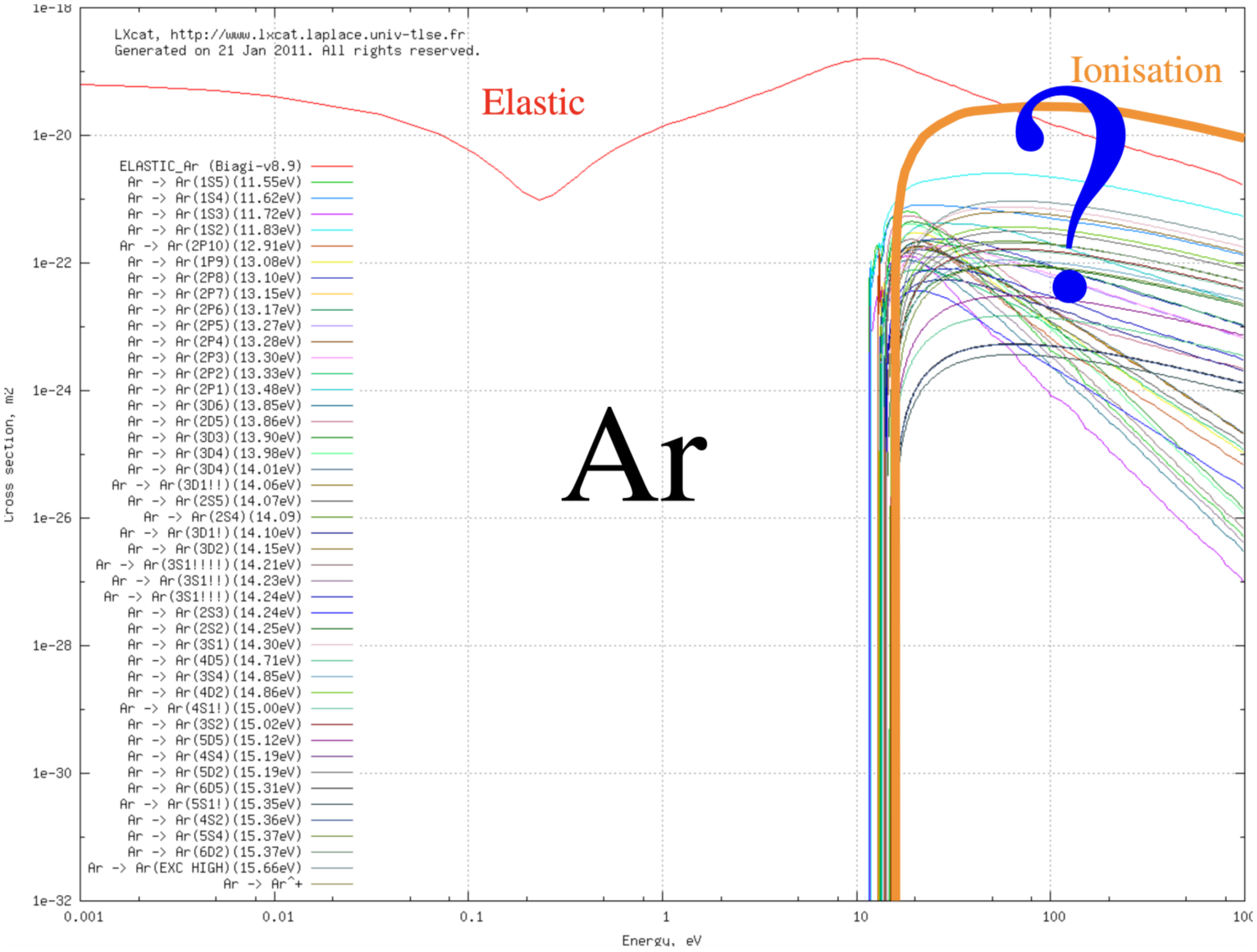

Microscopic Model

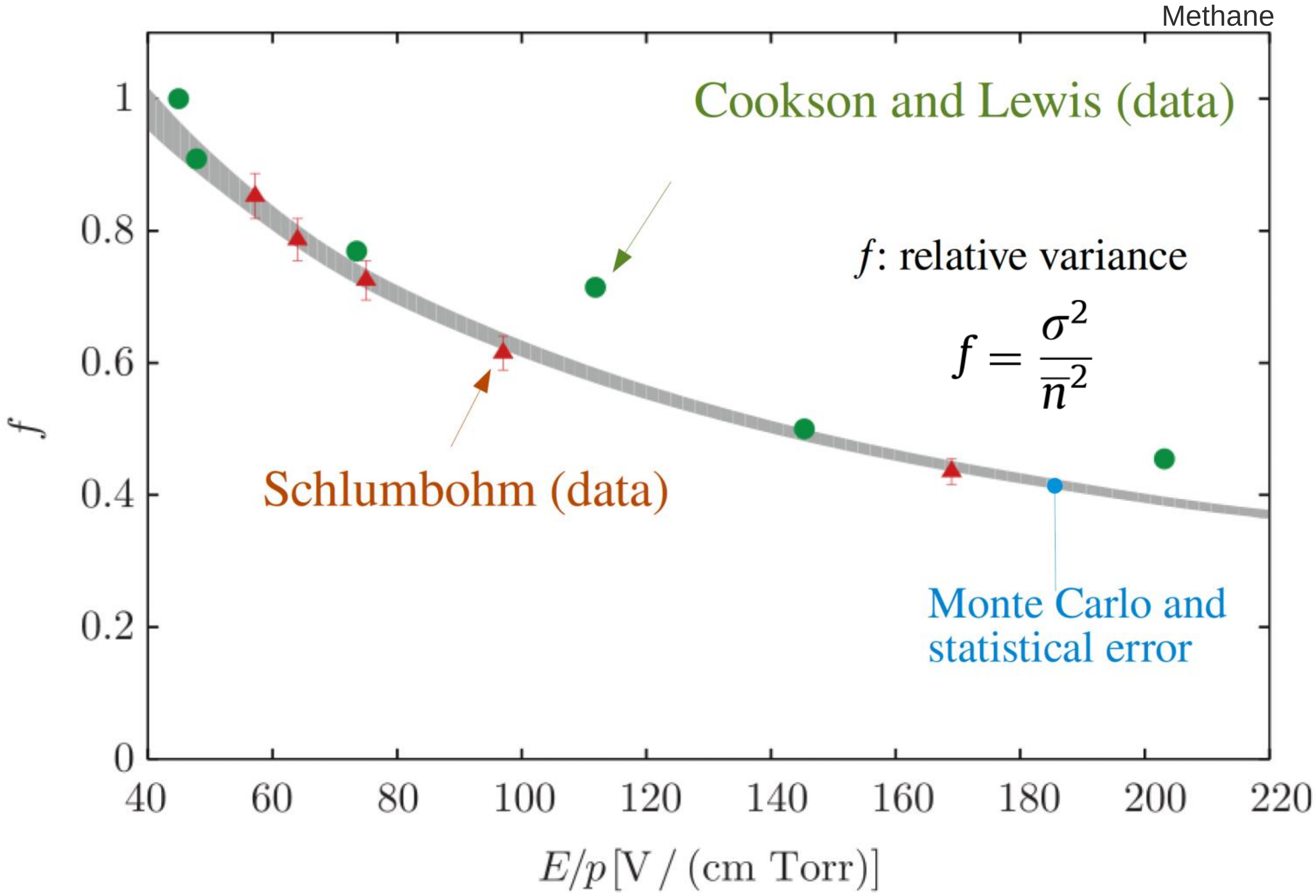

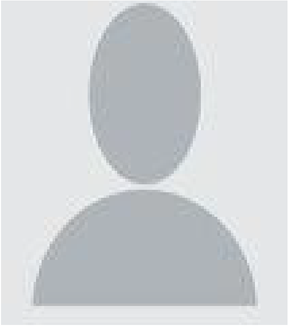

Stephen Biagi (MAGBOLTZ)

Rob Veenhof (Garfield/Garfield++)

Heinrich Schindler (Garfield++)

H. Schindler, S.F. Biagi, R. Veenhof, NIM-A 624 (2010) 78–84.

Example: Micromegas

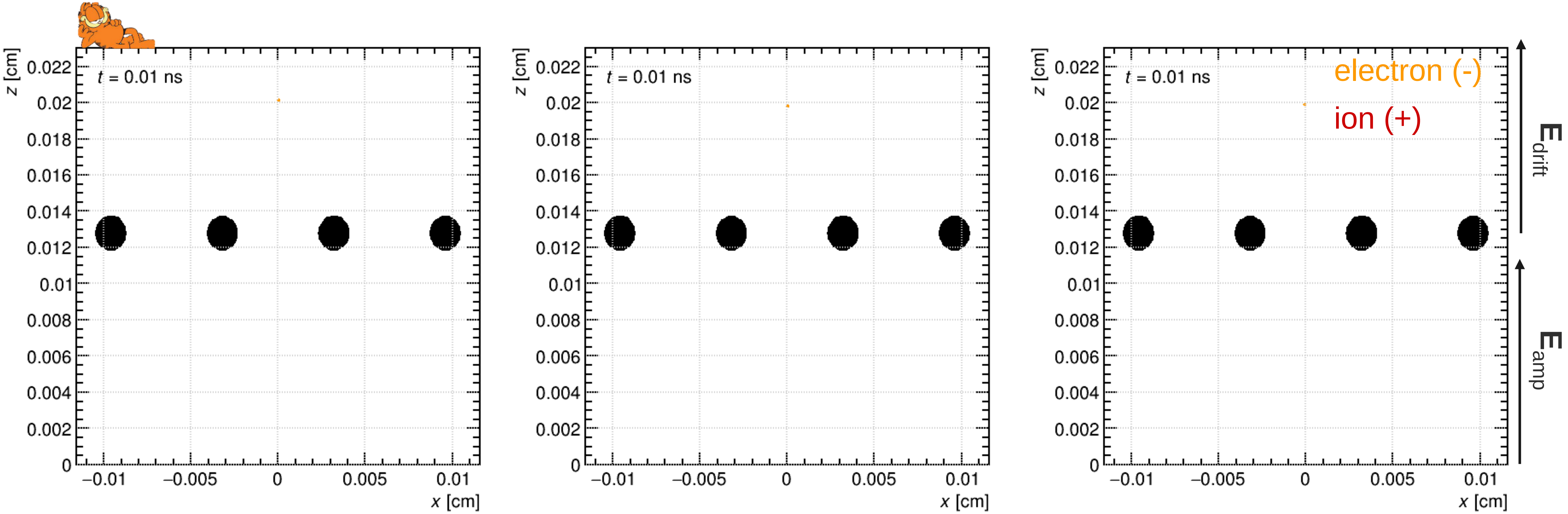

Microscopic Model

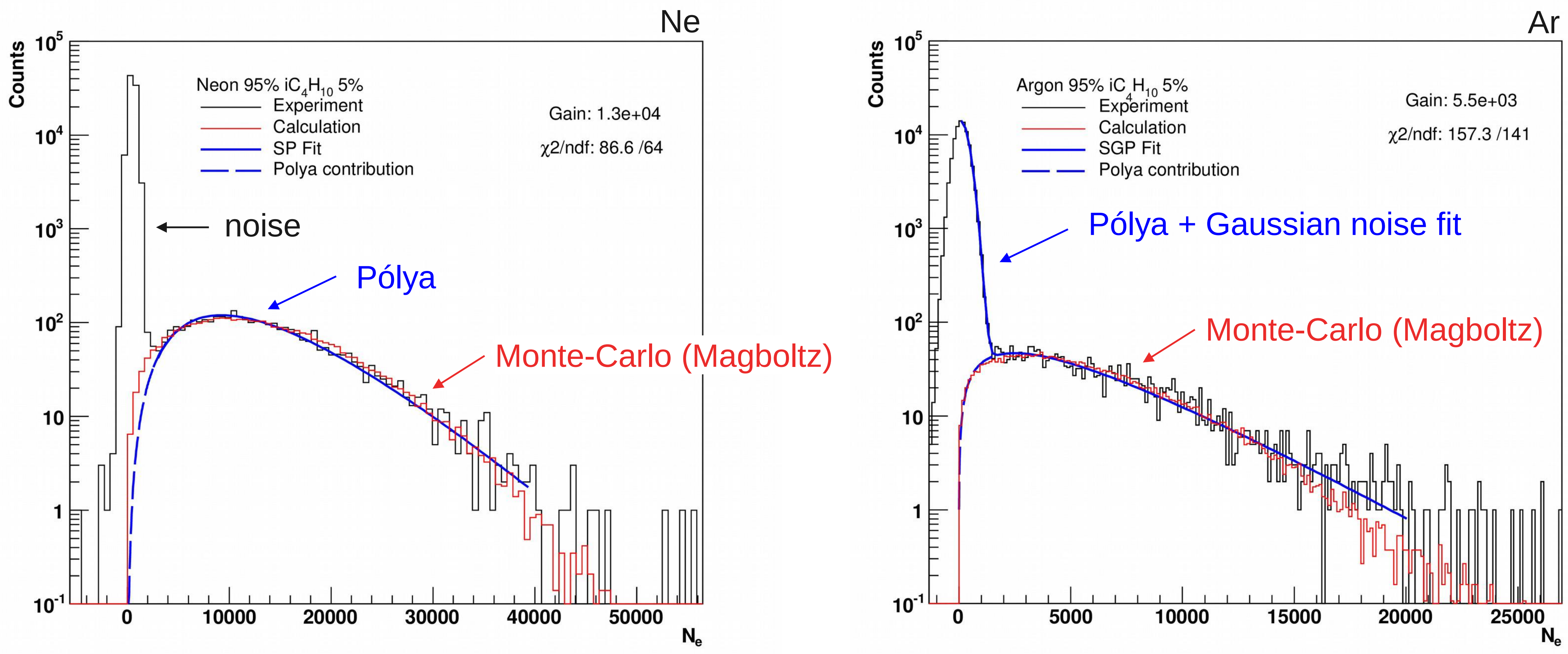

S. Biagi, Magboltz: https://magboltz.web.cern.ch/magboltz/.

Pólya Distribution

Running the simulation more then 800 times for a µRWELL, we can get the average avalanche size. The resulting non-monotonic “rounded” spectrum can be phenomenologically described by the Pólya distribution:

$$\overline{n}P_n = \frac{(\theta+1)^{\theta+1}}{\Gamma(\theta+1)}\left(\frac{n}{\overline{n}}\right)^{\theta} \mathrm{e}^{-(\theta+1)n/\overline{n}}$$

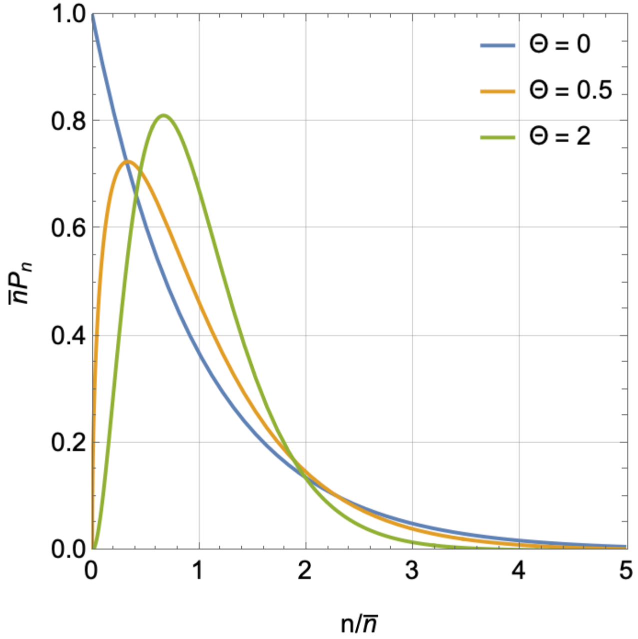

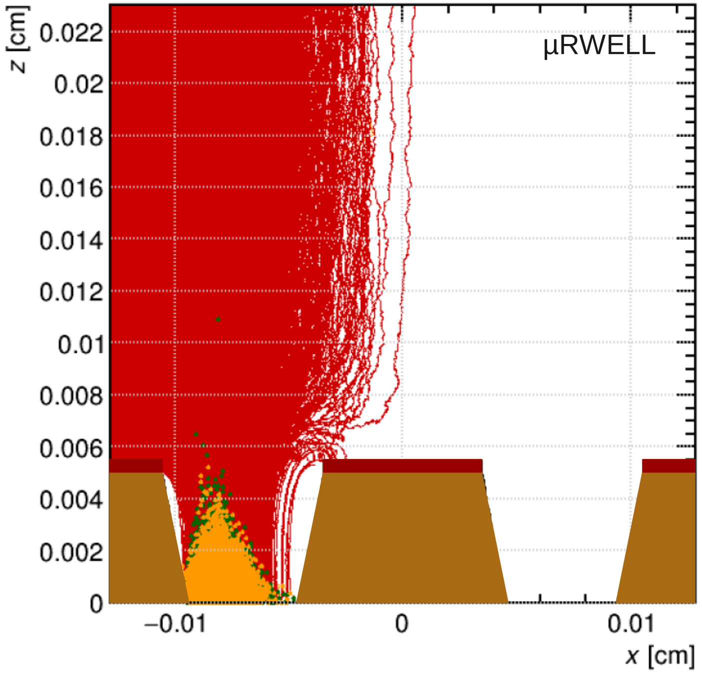

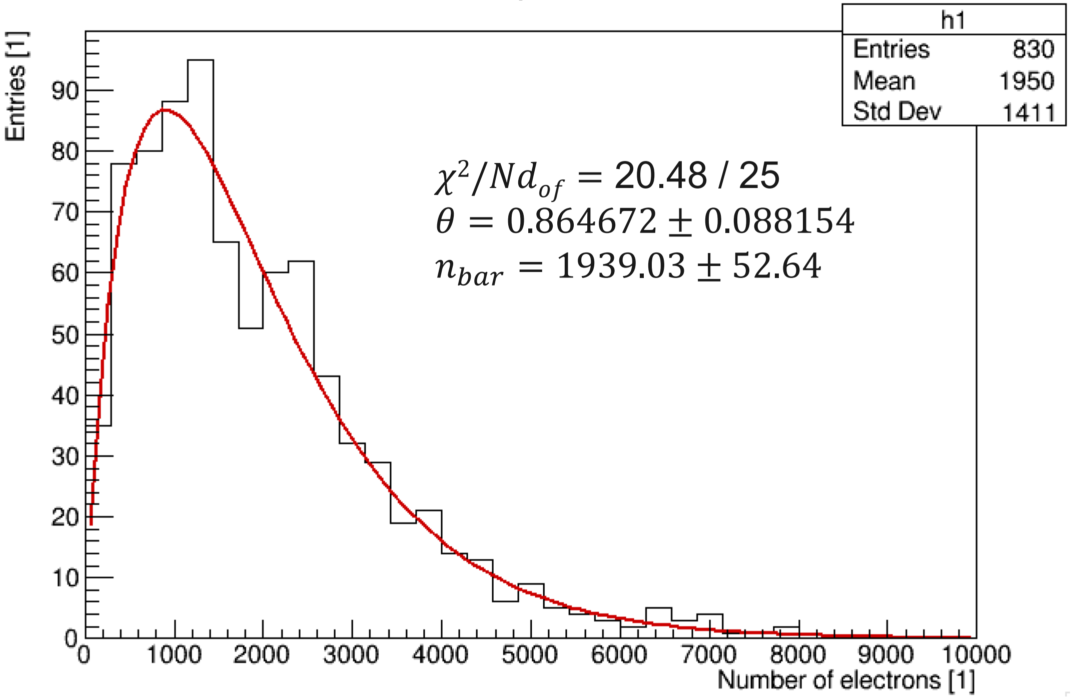

W. Legler, British Journal of Applied Physics 18 (1967) 1275.
A.C. S.C. Curran and J. Angus, The London, Edinburgh, and Dublin Philosophical Magazine and Journal of Science 40 (1949) 929.
J. Byrne, Proceedings of the Royal Society of Edinburgh Section A: Mathematics 66 (1962) 33–41.
G. Alkhazov, , Nuclear Instruments and Methods 89 (1970) 155.

Hydrodynamical Approximation

Space-charge Effects for Large Avalanches

Garfield++ gives an accurate description of the amplification in the proportional regime, where all electrons and ions are being drifted independently. Given the large avalanche sizes that can be found in timing detectors, space-charge effects could play a role.

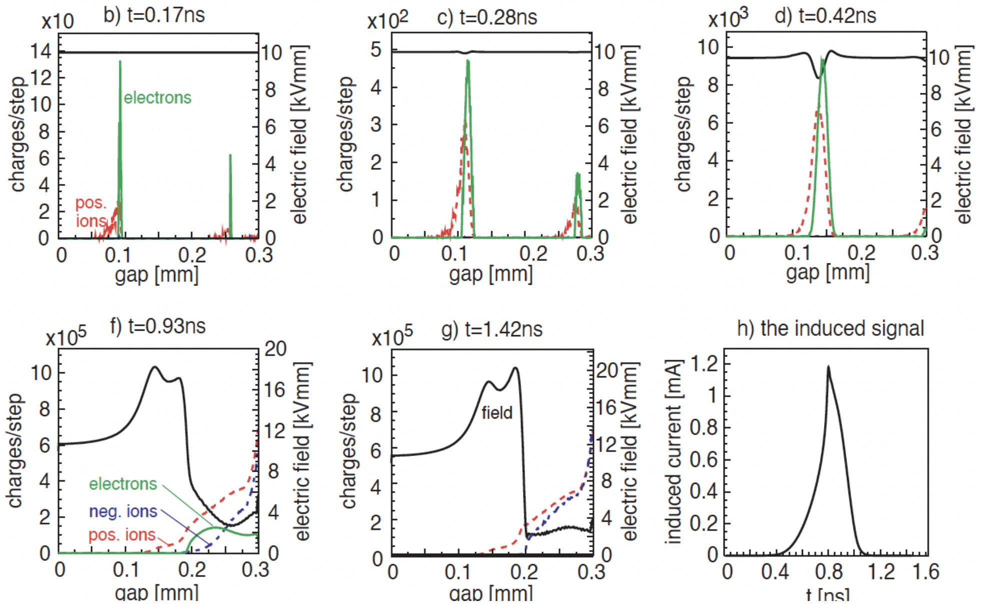

C. Lippmann, W. Riegler, NIM-A 517 (2004) 54–76.
See also presentation of Dario Stocco.

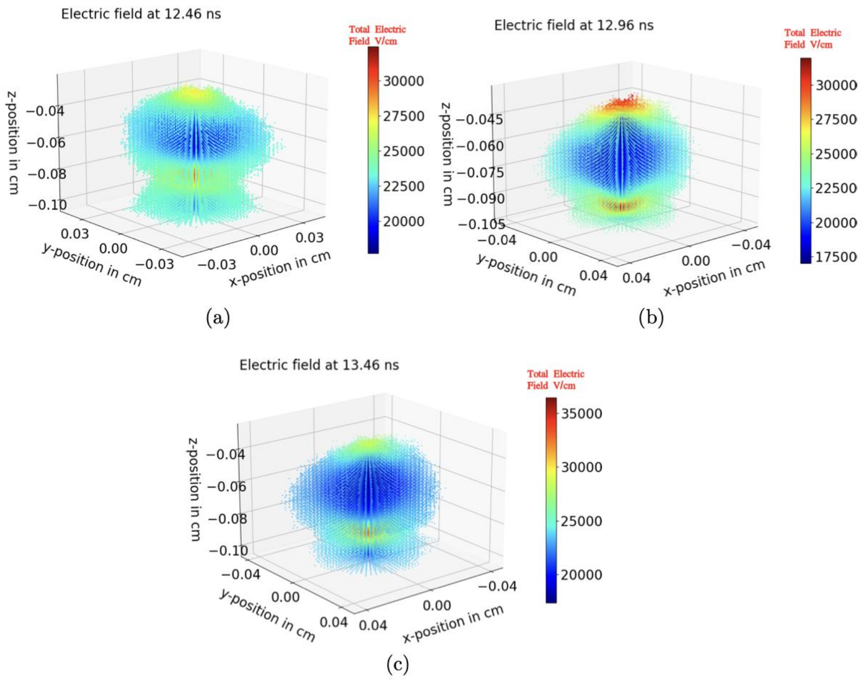

See presentation of Supratik Mukhopadhyay and Thursday's presentation given by Maxim Titov.
Also: arXiv:2211.06361v1 [physics.ins-det].

and more…

Hydrodynamical Approximation

We can approximate the number density of electrons and ions in the gas as “fluids” and describe their dynamics using advection diffusion reaction equation:

$$\overbrace{\frac{\partial n_e(\vec{r},t)}{\partial t} + \vec{\nabla}\cdot \underbrace{\left(\underset{transport}{\vec{W}_e n_e} - \underbrace{D_e \vec{\nabla} n_e}_{diffusion} \right)}_{electron\ flow\ density\ \vec{J}_e}}^{conservation} = \overbrace{\underset{\substack{other\\sources}}{S} + \underbrace{(\alpha-\eta)\left|\vec{J}_e\right|}_{\substack{multiplication\\-attachment}}}^{creation}$$

$n(\vec{r},t)$ = charge density in space and time

$\vec{W}_e(\vec{E})$ = velocity of electrons

$\vec{E}(\vec{r},t)$ = electric field: applied + space charge

α = first Townsend coefficient

η = attachment coefficient

D_e = diffusion coefficient

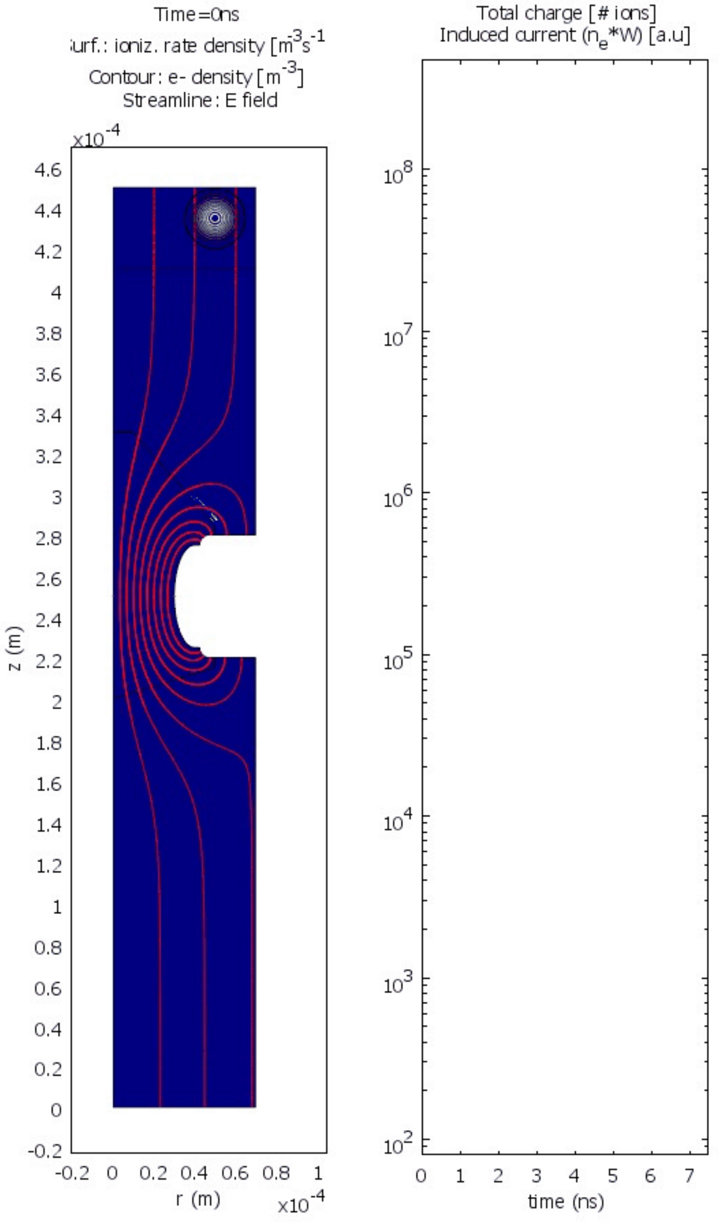

To include space-charge effects we can couple this to the Poisson equation

$$\nabla^2 V = -\frac{e}{\varepsilon_0}\left(n_{i+} - n_e - n_{i-}\right)$$

→ Deterministic model!

RD51–NOTE-2011-005, by Paulo Fonte.
RD-51 Open Lectures by Filippo Resnati.
Jaydeep Datta’s presentation.

S. Mukhopadhyay and P. Bhattacharya’s MPGD2024 contribution: https://indi.to/wym7w.
Equations taken from P. Fonte’s WG4 presentation: https://indi.to/9TWnL.

Hydrodynamical Approximation: Rate Dependence of GEM Gain

The gain modification of GEMs as a function of the rate can be reproduced using this kind of approach.

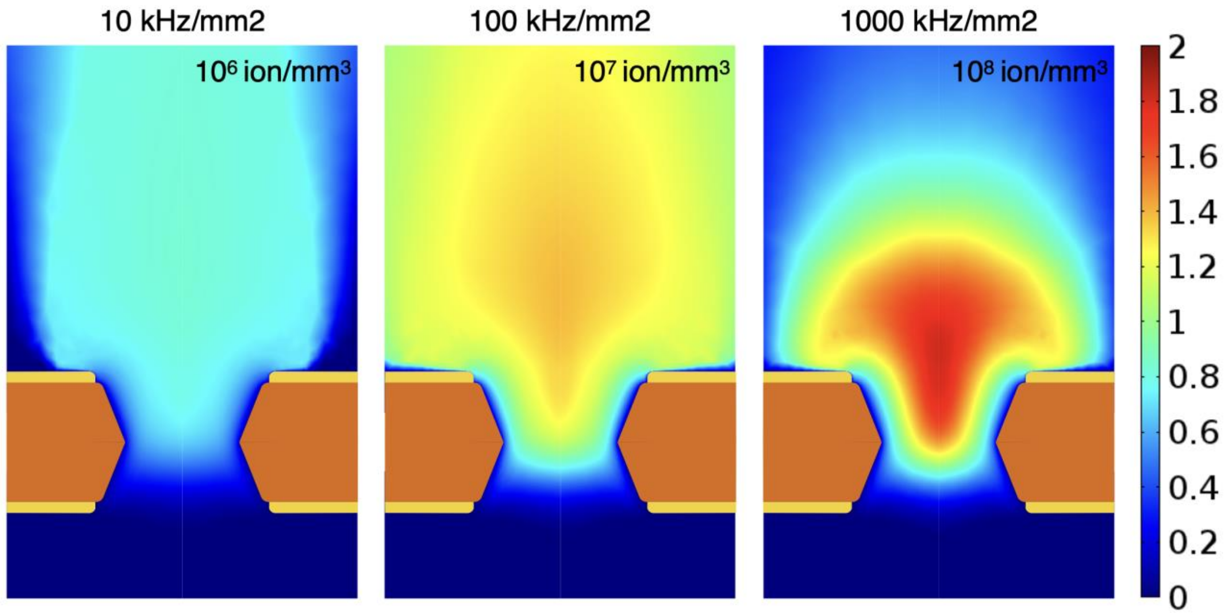

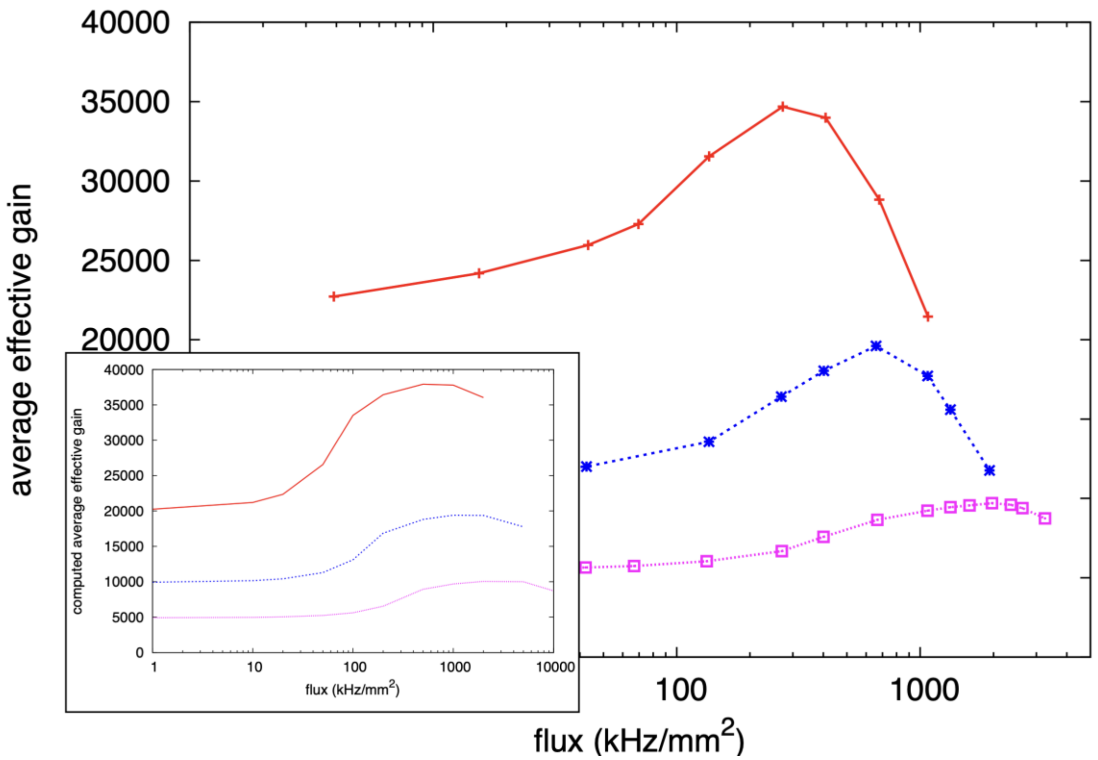

Hydrodynamical Approximation: Streamer in RPC

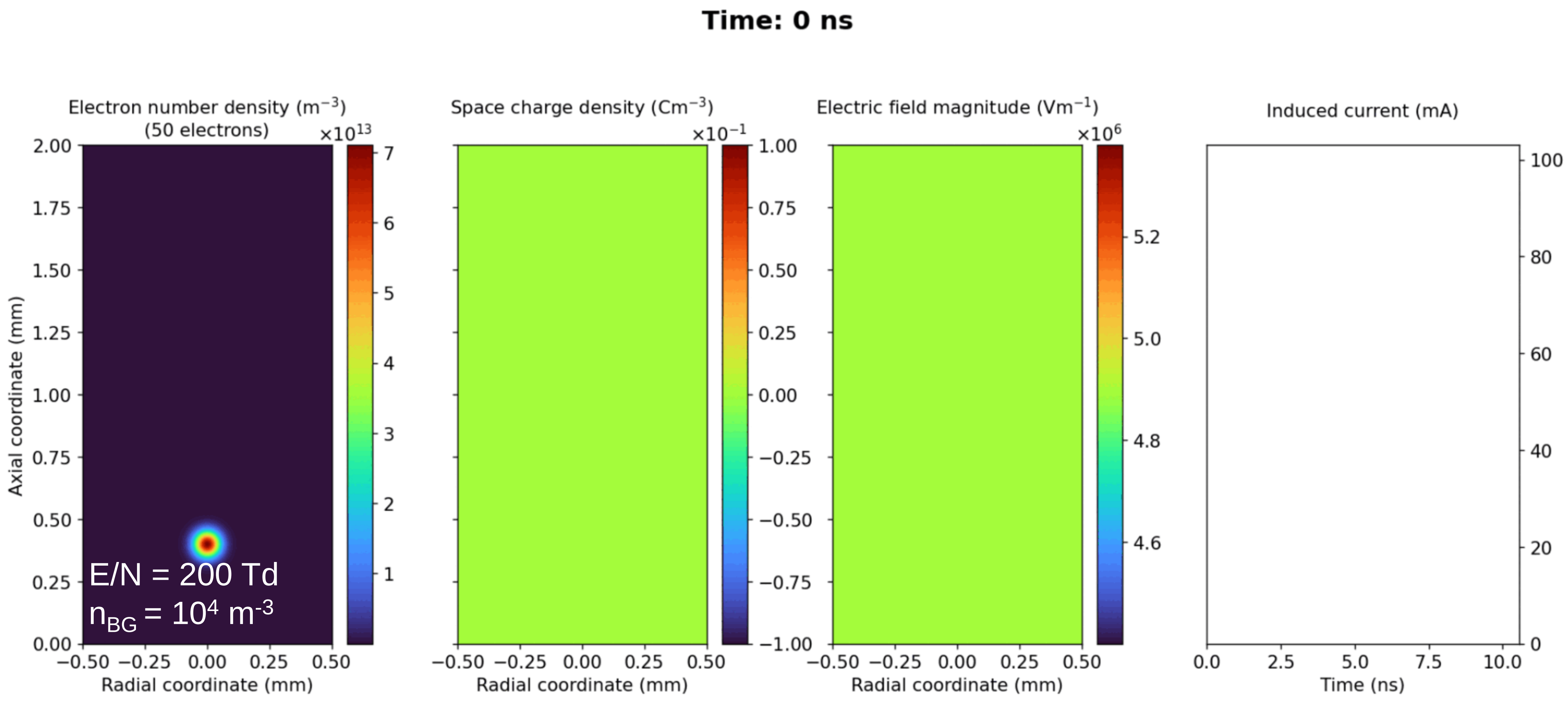

D. Bošnjaković, I. Simonović, and S. Dujko, presentation at RPC2024: https://indi.to/Sxg8j.

Intermediate Summary

We have seen different approaches to describe the avalanche dynamics in a gas medium.

- **Analytic models:** Can provide general insights through equation-based toy-models, given certain approximations.

- **Macroscopic models:** Can efficiently model the stochastic quantities using approximate models (Yule-Furry, Legler, ect.).

- **Microscopic model:** A model capturing the stochastic process in detail, but more computationally demanding, especially when dealing with large avalanches and space-charge effects.

- **Hydrodynamic approximation:** Deterministic model useful for large avalanche and space-charge effects simulations.

→ We can combine different methods to overcome some of their individual shortcomings!

Capacitive Coupling Between Electrodes

Capacitive Coupling Between Electrodes

The cross-talk between the bottom of the GEM foil and readout needed to be considered in the LHC experiments in various instances.

ALICE TPC

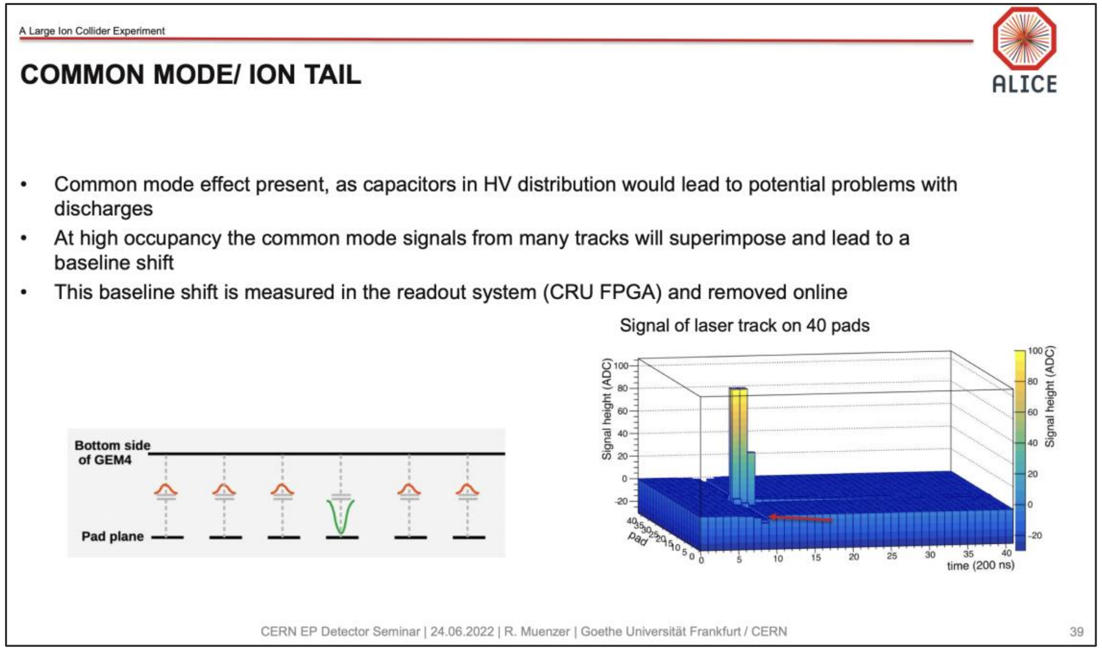

Slide borrowed from R. Münzer's Detector Seminar

CMS GEM

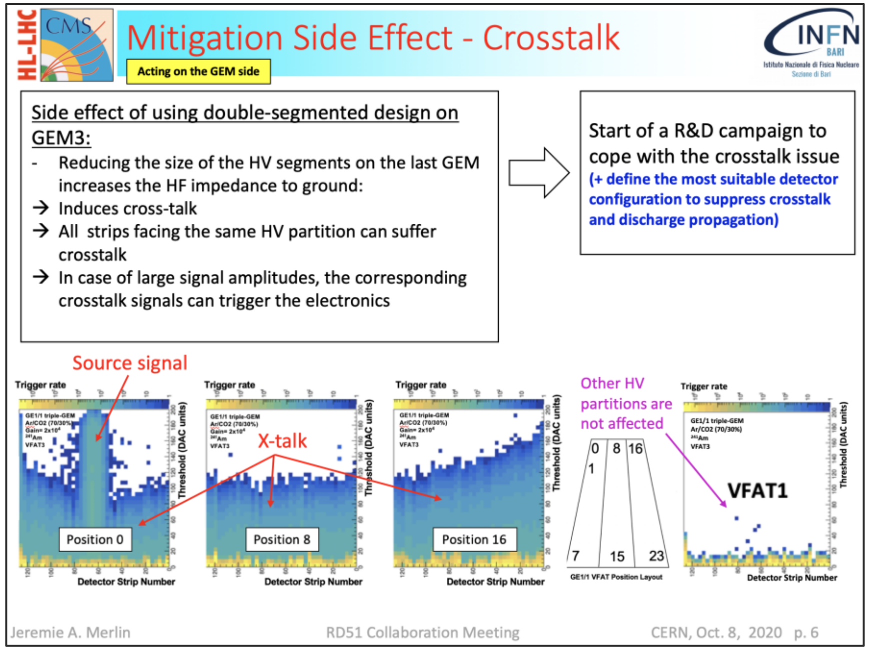

Slide borrowed from J.A. Merlin's contribution to the RD51 Coll. Meetings.

See also the LHCb blocking capacitor of the GEM muon system.

Capacitive Coupling Between Electrodes

For a PICOSEC-like MM setup, the Finite Element Method was used to calculate both the weighting potentials for all three electrodes, and the applied electric field.

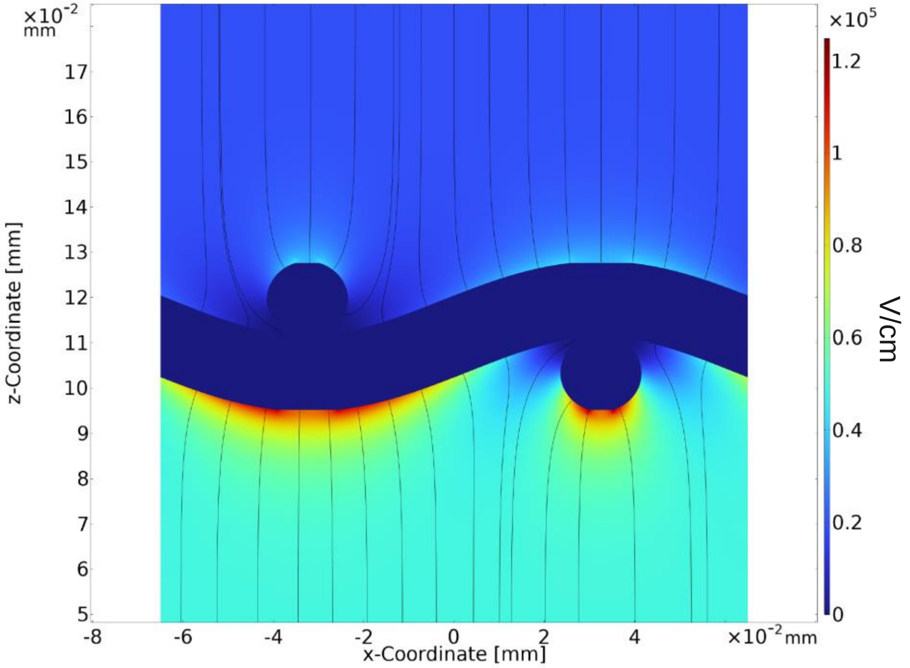

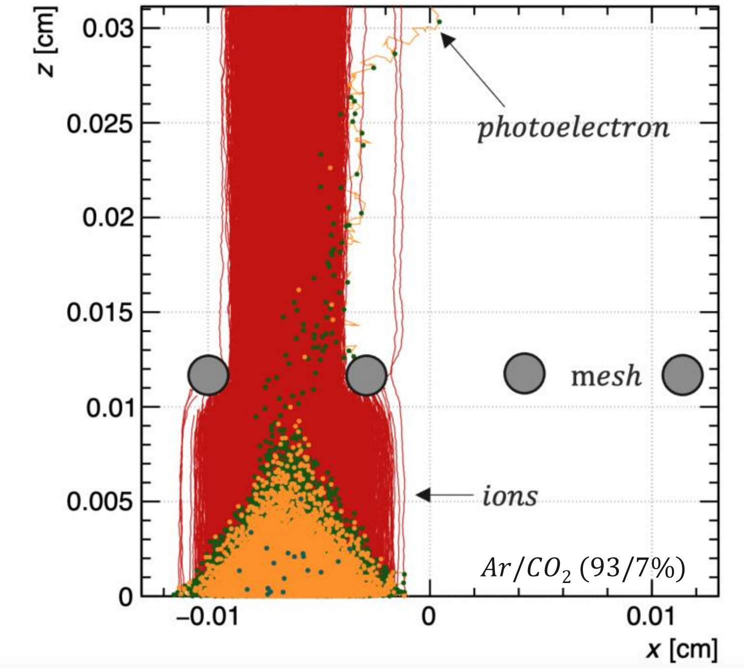

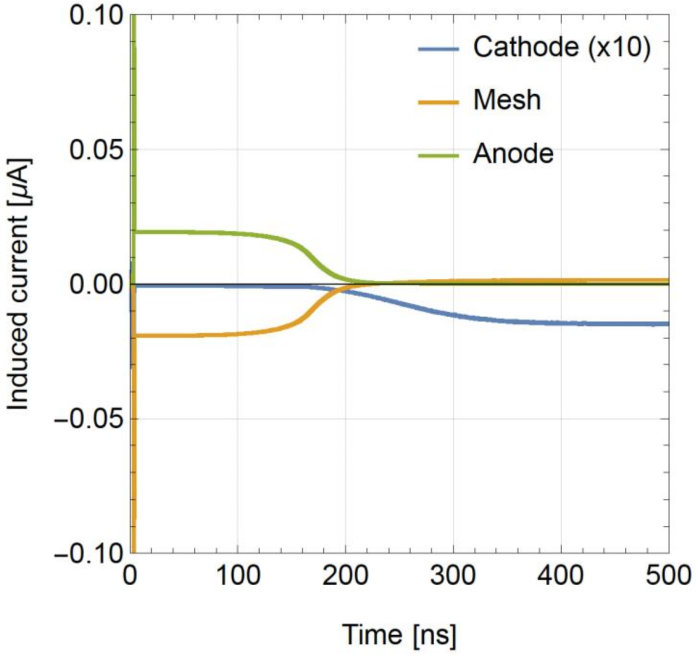

Capacitive Coupling Between Electrodes

Typically, the detector is equipped with external impedance elements, such as HV dividers, noise filters, amplifiers, etc.

Laplace parameter

$$\frac{I_3}{I_0} = \frac{sC_3}{s\left(\frac{C}{sCR_1+1} + C_3\right) + \frac{1}{R_2}}$$

To understand how this changes the final signal, the induced signals can be seen as an ideal current source in an equivalent circuit.

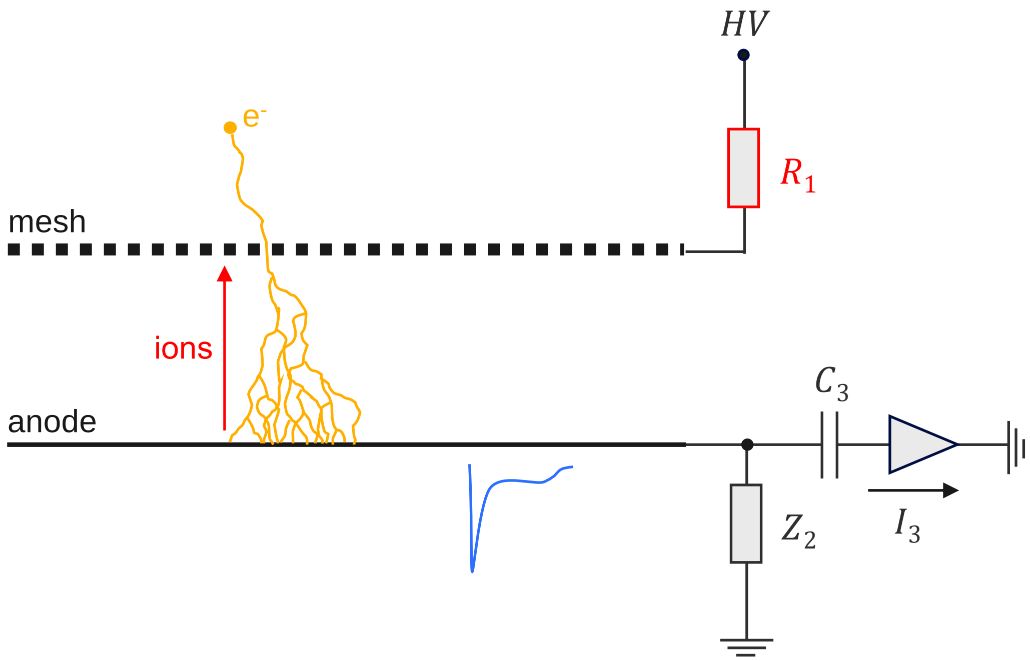

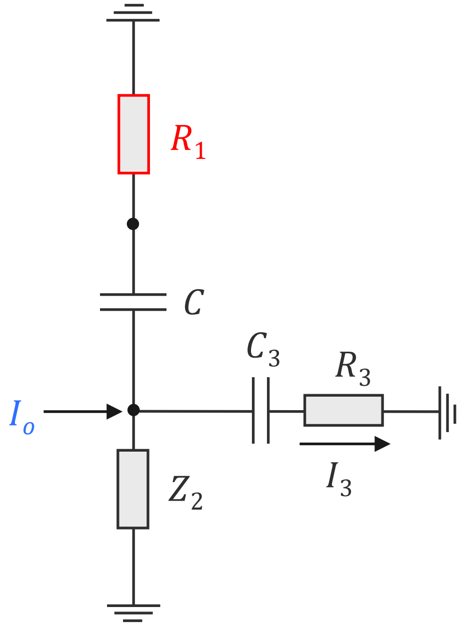

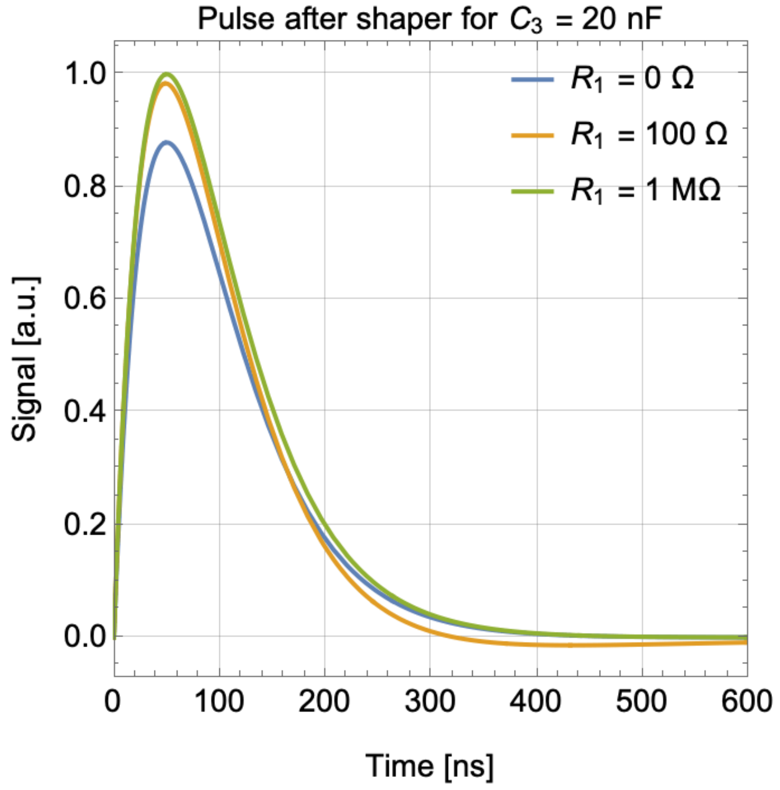

Here we take $Z_2 = 100\ M\Omega$.

Capacitive Coupling Between Electrodes

Induced signals can couple to other (neighboring) electrodes due to their mutual capacitance. Increasing R_1 forces the mesh current to couple to the anode.

$$\frac{I_3}{I_0} = -\frac{s^2 C C_3 R_1 R_2}{sC(sC_3 R_1 R_2 + R_1 + R_2) + sC_3 R_2 + 1}$$

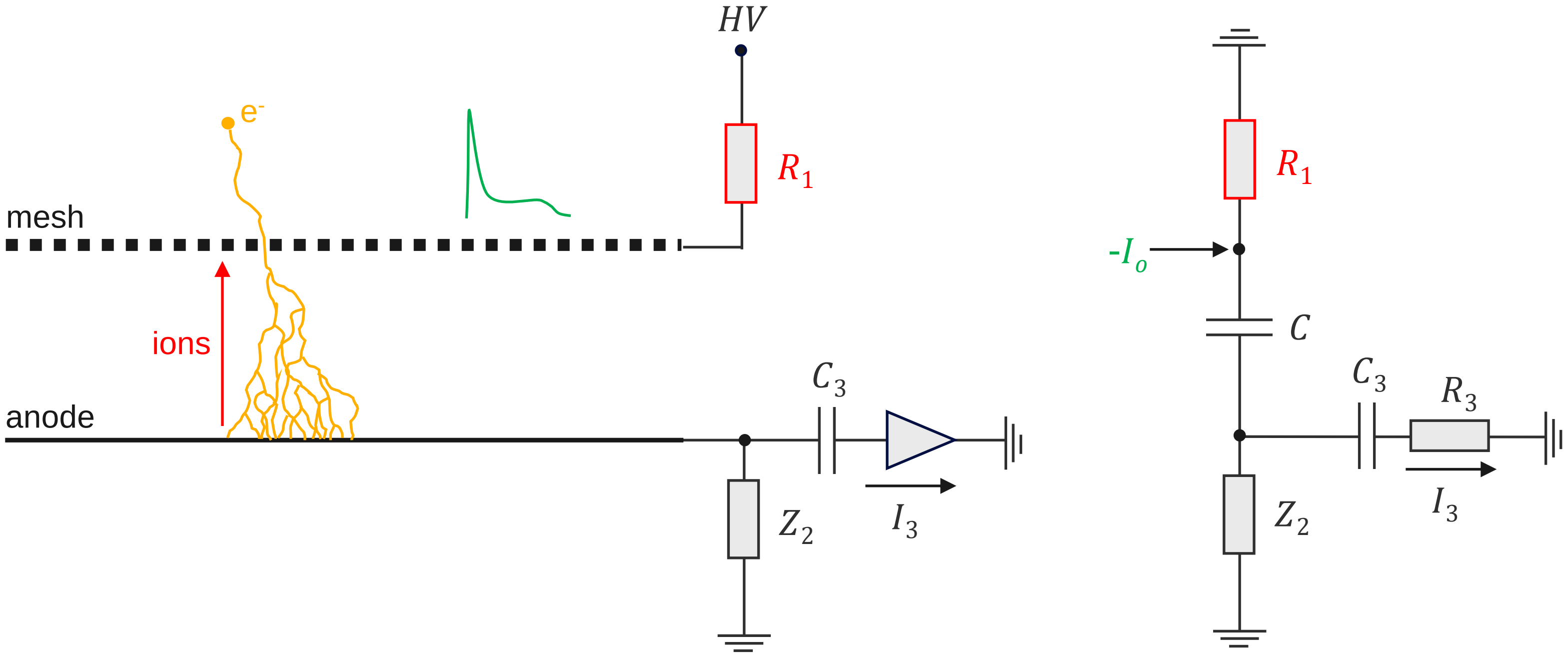

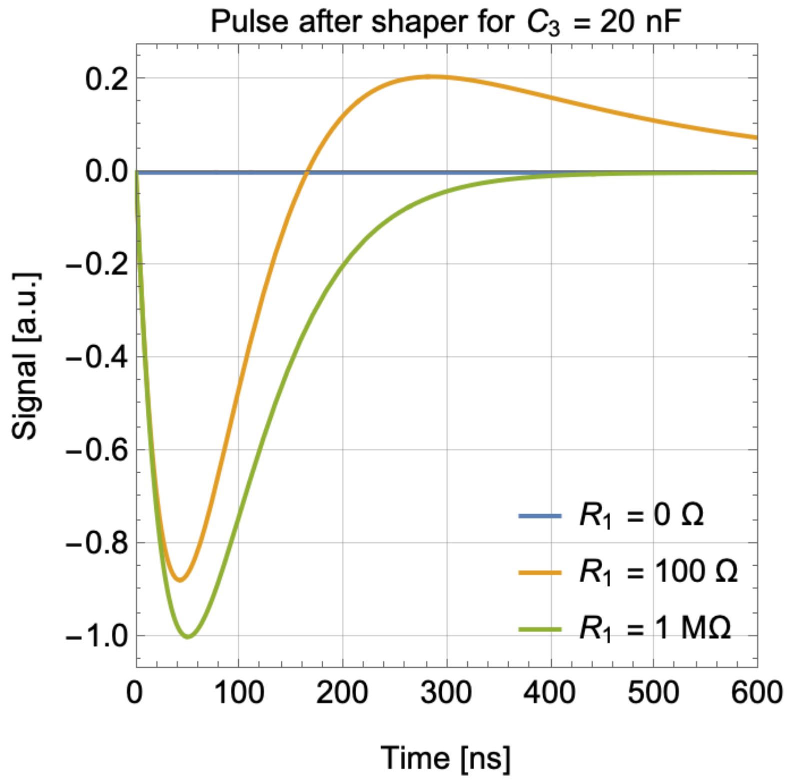

Here we take $Z_2 = 100\ M\Omega$.

Capacitive Coupling Between Electrodes

Given the opposite polarity of the mesh and anode current, increasing R_1 starts to 'cancel' out the signal read from the anode.

$$\frac{I_3}{I_0} = \frac{sC_3R_2}{1 + sC_3R_2 + sC(R_1 + R_2 + sC_3R_1R_2)}$$

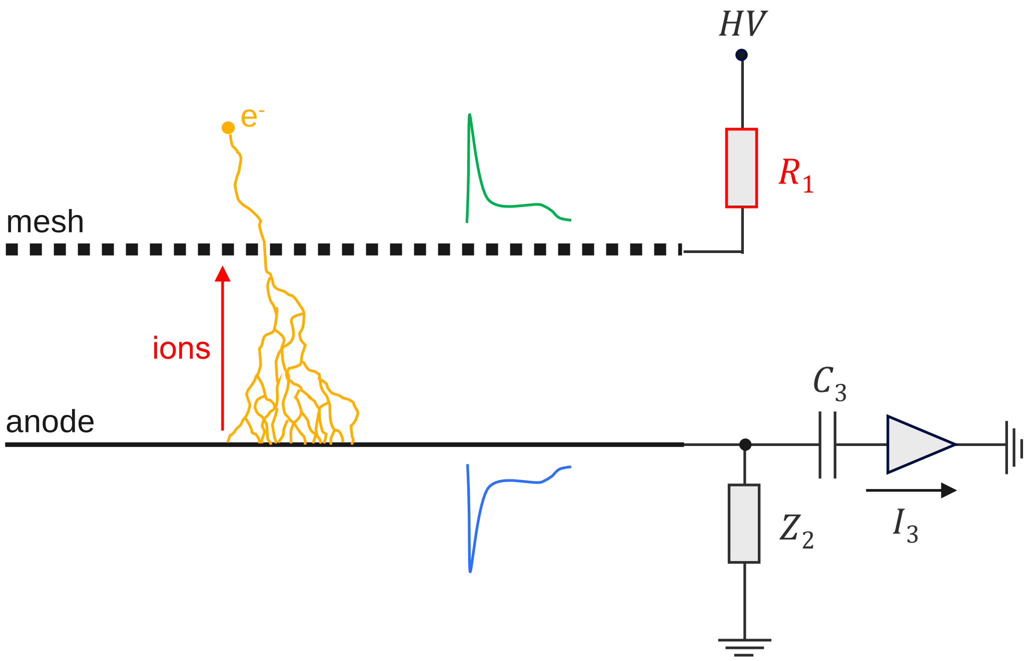

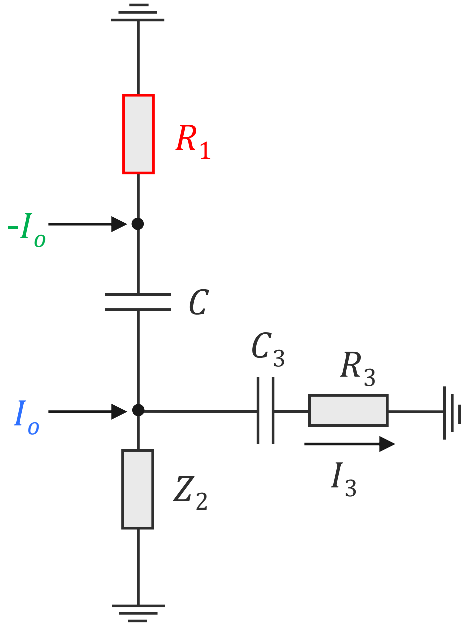

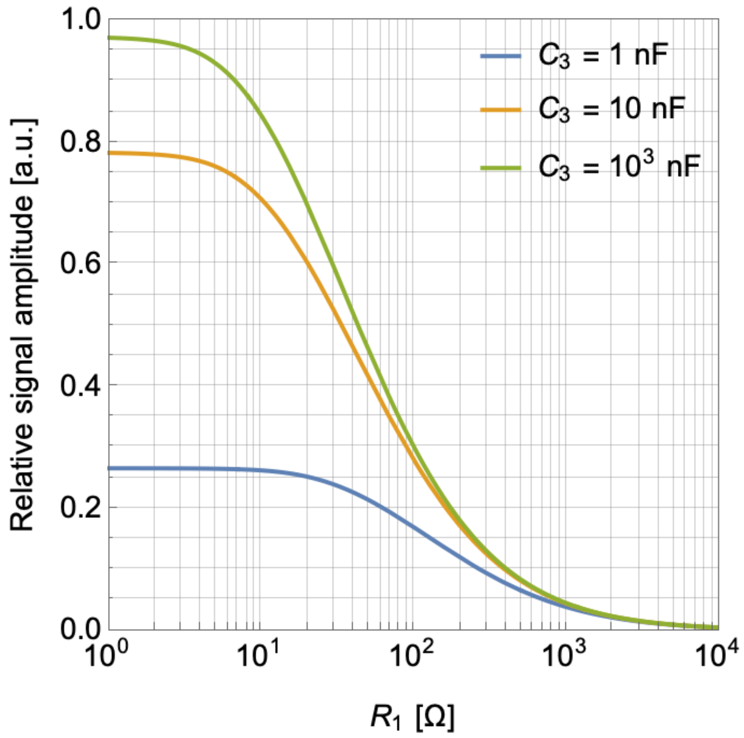

Here we take $Z_2 = 100\ M\Omega$.

Capacitive Coupling Between Electrodes

This can be overcome by introducing a blocking capacitor C_b, offering a low impedance path to ground for the mesh current.

$$\frac{I_3}{I_0} = \frac{sC_bR_1 + 1}{sC(sR_1R_2(C_3 + C_b) + R_1 + R_2) + (sC_3R_2 + 1)(sC_bR_1 + 1)}$$

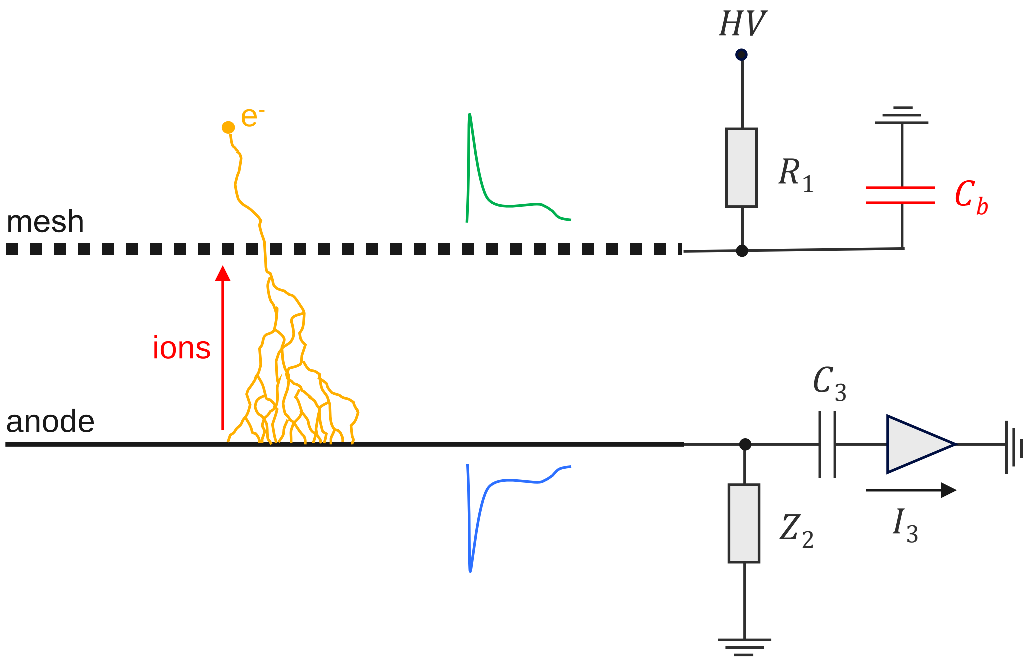

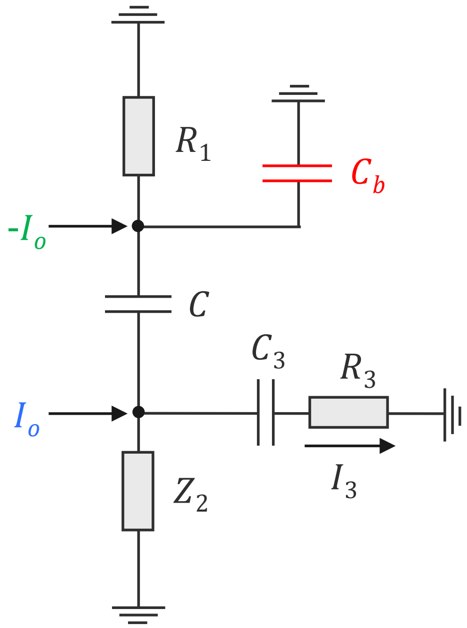

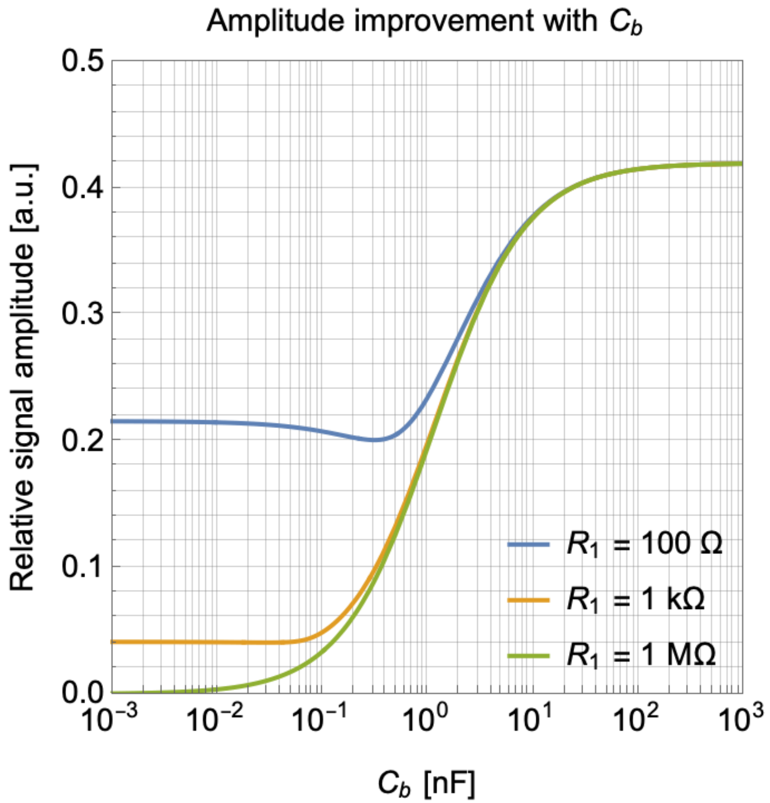

Here we take $Z_2 = 100\ M\Omega$.

Capacitive Coupling Between Electrodes

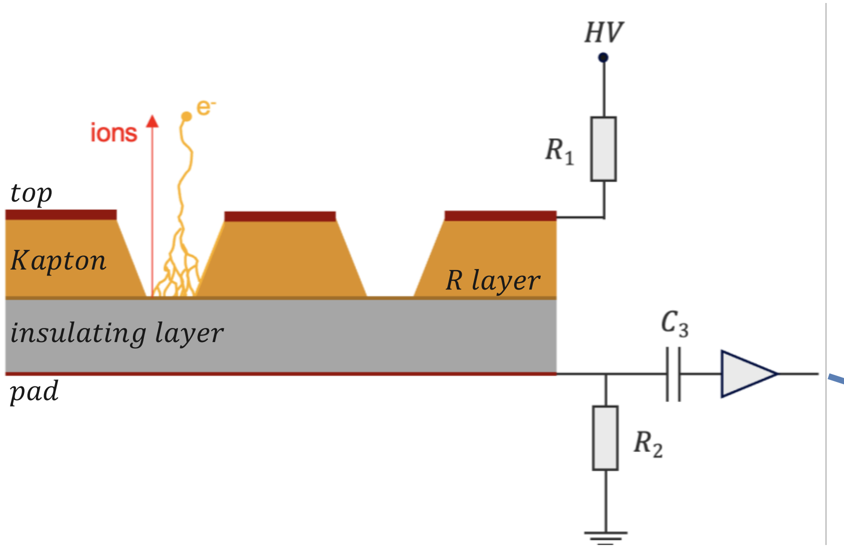

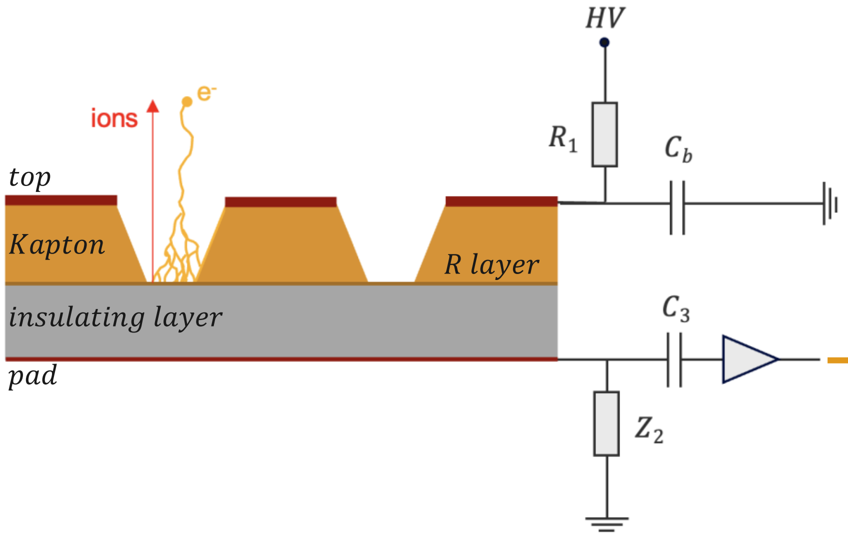

Including the blocking capacitor C_b can improve the signal amplitude on the readout plane due to its low impedance path to ground for the top signal.

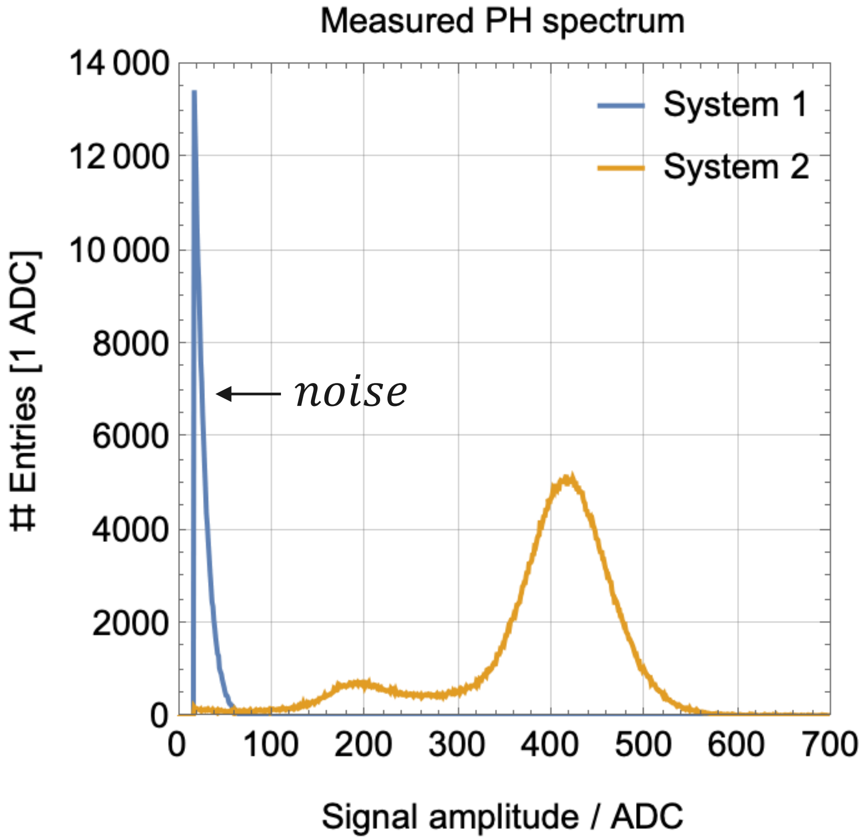

Capacitive Coupling Between Electrodes

When the anode is segmented in N electrodes, the induced signal on the mesh is coupled to all individual channels, giving, by approximation, a similar effect as the blocking capacitor of before.

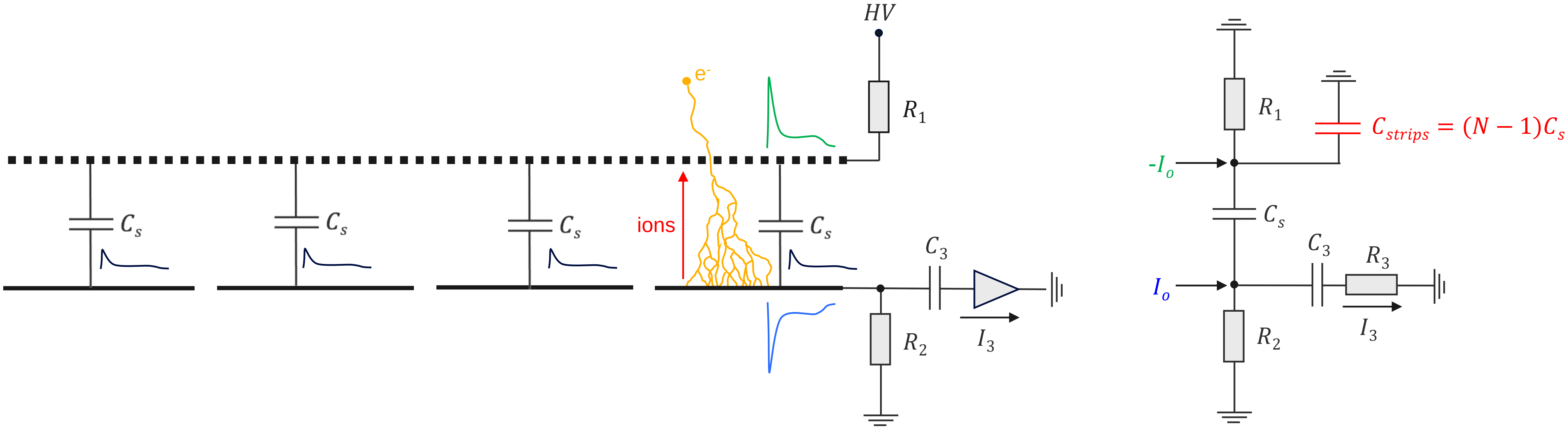

Capacitive Coupling Between Electrodes

There is a capacitive coupling between the readout electrodes. To calculate all mutual capacitances, we can use a Finite Element Solver (FEM) to obtain the Maxwell capacitance matrix.

µRWELL with 2D strip readout

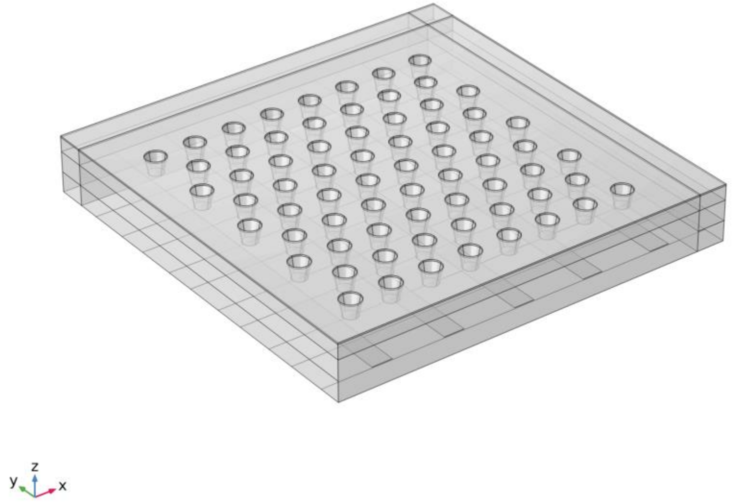

Meshed geometry to be solved using FEM

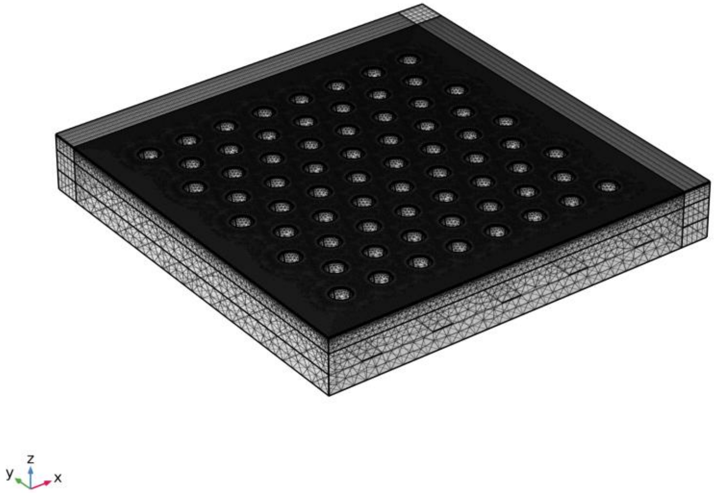

Mutual capacitance matrix

$$\begin{pmatrix}
-0.2904 & 29.7096 & 0.0003 & 0.0003 & 0.0003 & 0.1027 & 0.0001 & 0.0001 & 0.0001 & 0.0072 \\
29.6489 & -2.0335 & 3.5516 & 3.5727 & 3.5576 & 3215.08 & 0.0225 & 0.0228 & 0.0221 & 26.1602 \\
-0.0026 & 3.5402 & 0.0179 & 0.0205 & 0. & 0.227 & 0.0143 & 0.0142 & 0.0143 & 30.8085 \\
-0.0024 & 3.5625 & 0.0205 & 0.0152 & 0.0204 & -0.0016 & 0.0144 & 0.0142 & 0.0144 & 30.9901 \\
-0.003 & 3.5445 & 0. & 0.0204 & 0.0206 & 0.2265 & 0.0143 & 0.0142 & 0.0143 & 30.8596 \\
-0.0923 & 3214.55 & 0.2323 & 0.0027 & 0.2323 & -0.1196 & 105.248 & 105.035 & 105.249 & 27627.5 \\
0. & 0.0219 & 0.0143 & 0.0144 & 0.0143 & 105.248 & -0.0003 & 0.2537 & 0. & 0.0605 \\
-0.0001 & 0.0221 & 0.0142 & 0.0142 & 0.0142 & 105.034 & 0.2537 & -0.0001 & 0.2537 & 0. \\
-0.0083 & -0.012 & 0.0143 & 0.0144 & 0.0143 & 105.231 & 0. & 0.2537 & 0.06 & 0.0602 \\
0.0344 & 26.2476 & 30.8087 & 30.9902 & 30.8597 & 27627.5 & 0.0605 & 0. & 0.0612 & -0.2995
\end{pmatrix}$$

Subsequently, a circuit solver like LTSpice can be used to solve the equivalent circuit.

COMSOL Multiphysics: https://www.comsol.com
LTSpice: https://www.analog.com/en/resources/design-tools-and-calculators/ltspice-simulator.html

Impedance Between Terminals

When working with resistive materials, the voltages and currents between the terminals are related through the admittance matrix.

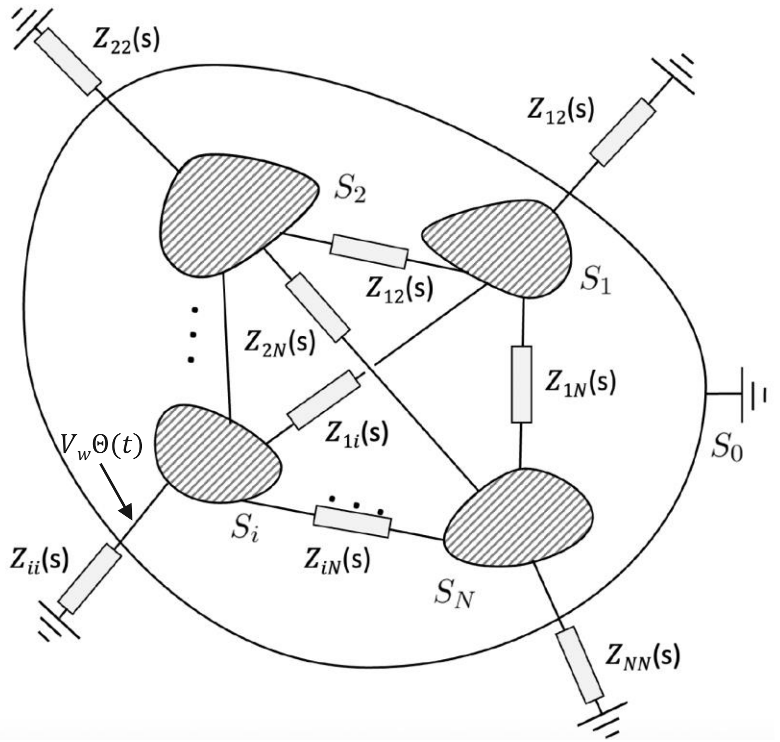

Given external impedance elements connected to our terminals, we can view them 'as part of the detector medium'.

$$I_i(t) = -\frac{q}{V_w}\int_0^t \mathbf{H}_i^*\left[\mathbf{x}_q(t'), t-t'\right]\cdot\dot{\mathbf{x}}_q(t')\,dt'$$

The dynamic $\psi_i^*(\mathbf{x}, t)$ can be calculated for a connected electrode using the following steps:

- Remove the drifting charges
- Connect the external circuit to the terminals
- Put a potential V_w at time t = 0 at the point where you want to know the signal

E. Gatti, G. Padovini and V. Radeka, Nuclear Instruments and Methods in Physics Research 193 (1982) 651.
W. Riegler, Nucl. Instrum. Meth. A 535 (2004), 287-293.
W. Riegler, Signals in Particle Detectors, CERN's Academic Training Lecture (2019).

Summary

- Microscopic tracking allows for an accurate description of the avalanche size distribution, and by extension, the stochastic quantities of the detector (energy resolution, etc.). It does not require any simplifying assumption about the ionization distance of the electrons, such as those found in the macroscopic Yule-Furry and Legler models.

- Approximating the electron and ion number densities as fluids, their evolution and modification of the electric field can be described using the advection diffusion reaction equation and Poison equation in a deterministic way.

- The induced currents on the readout electrodes can be calculated using (time-dependent) weighting potentials. To describe the capacitive coupling between terminals, these currents should be injected into the equivalent circuit of the detector system, or the external impedance elements can already be included into the dynamic weighting potential.

Thank you for your attention!